Hindawi
Wireless Communications and Mobile Computing
Volume 2021, Article ID 9915420, 25 pages
https://doi.org/10.1155/2021/9915420

Research Article

A Novel Modified Sparrow Search Algorithm with Application in Side Lobe Level Reduction of Linear Antenna Array

Qiankun Liang,[1] **Bin Chen**,[1] **Huaning Wu**,[1] **Chaoyi Ma**,[2] **and Senyou Li**[2]

[1]*Naval University of Engineering, College of Electronic Engineering, Wuhan 430033, China*
[2]*China Academy of Information and Communications Technology, Beijing 100191, China*

Correspondence should be addressed to Huaning Wu; wuhuaning007@163.com

Received 18 March 2021; Revised 17 May 2021; Accepted 4 June 2021; Published 28 June 2021

Academic Editor: Fawad Zaman

Antenna arrays play an increasingly important role in modern wireless communication systems. However, how to effectively suppress and optimize the side lobe level (SLL) of antenna arrays is critical for communication performance and communication capabilities. To solve the antenna array optimization problem, a new intelligent optimization algorithm called sparrow search algorithm (SSA) and its modification are applied to the electromagnetics and antenna community for the first time in this paper. Firstly, aimed at the shortcomings of SSA, such as being easy to fall into local optimum and limited convergence speed, a novel modified algorithm combining a homogeneous chaotic system, adaptive inertia weight, and improved boundary constraint is proposed. Secondly, three types of benchmark test functions are calculated to verify the effectiveness of the modified algorithm. Then, the element positions and excitation amplitudes of three different design examples of the linear antenna array (LAA) are optimized. The numerical results indicate that, compared with the other six algorithms, the modified algorithm has more advantages in terms of convergence accuracy, convergence speed, and stability, whether it is calculating the benchmark test functions or reducing the maximum SLL of the LAA. Finally, the electromagnetic (EM) simulation results obtained by FEKO also show that it can achieve a satisfactory beam pattern performance in practical arrays.

1. Introduction

The latest development trend of wireless communication systems is to realize the antenna array system with strong directivity and maneuverability, so that it can radiate and receive energy to the maximum extent in a specific direction and reduce the waste of energy by suppressing the SLL in noninteresting directions [1]. According to the pattern multiplication theorem, the pattern of an antenna array can be obtained by multiplying the element pattern by the array factor. By adjusting the spacing, excitation amplitude, and phase of array factor, the antenna array can have the characteristics of high gain, narrow beam, low SLL, and easy electrical scanning [2]. In the field of scientific research and engineering practice, most of the problems encountered can be attributed to solving optimization problems, and the design and optimization of the antenna array are no exception [3]. With the development of computer technologies and computational electromagnetics, some intelligent optimization algorithms that simulate the behavior mechanism of biological groups or the laws of natural phenomena have begun to appear in the vision of many scholars. With its unique advantages in solving large-scale, nonlinear, and other complex optimization problems, the design and optimization technology of antenna arrays based on an intelligent optimization algorithm has always been a research hotspot in the field of EM optimization [4].

In the past few decades, various intelligent optimization algorithms have been implemented to optimize and design antenna arrays, such as genetic algorithm (GA) [5], particle swarm optimization (PSO) [6], bees algorithm (BA) [7], biogeography-based optimization (BBO) [8], firefly algorithm (FA) [9], cat swarm optimization (CSO) [10], cuckoo optimization algorithm (COA) [11], backtracking search algorithm (BSA) [12], symbiotic organisms search (SOS) [13], grey wolf optimization (GWO) [14], extended GWO (GWO-E) [15], spider monkey optimization (SMO) [16], gravitational search algorithm (GSA) [17], invasive weed

optimization (IWO) [18], elephant swarm water search algorithm (ESWSA) [19], grasshopper optimization algorithm (GOA) [20], and equilibrium optimization algorithm (EOA) [21]. These algorithms have been successfully applied in this field. However, according to no free lunch (NFL) theorem, no algorithm can perform best on all kinds of optimization problems [22]. Therefore, finding and researching more efficient algorithms are still a problem worthy of attention in the field of EM optimization.

SSA is a new intelligent optimization algorithm proposed by Xue and Shen in 2020. It is mainly inspired by the foraging and antipredation behaviors of sparrows. It has the characteristics of simple implementation, few adjustment parameters, and high expansibility and has been successfully applied in many scientific research and engineering practice fields [23]. For example, [24] proposed an improved SSA to solve the path planning problem of UAV under constraint and proved that the route generated by this method is better than that by the other four algorithms in the same environment. Wang and Xianyu used SSA to solve the optimal configuration model of distributed power supply for the first time and verified the effectiveness and superiority of this method through the IEEE 33 distribution system [25]. Reference [26] established the SSA model based on empirical mode decomposition to optimize the parameters of the kernel extreme learning machine (KELM) and achieved higher prediction accuracy in blood glucose prediction. Kumaravel and Ponnusamy improved the control parameters of the power controller based on SSA to optimize the power flow management of the smart grid system, which realized the real-time energy management in the microgrid [27]. In [28], the improved model based on SSA can track the distributed maximum power point more accurately and quickly and has good robustness, thus effectively solving the problem of power mismatch loss in a photovoltaic microgrid system. Zhu and Yousefi introduced an adaptive strategy on the basis of SSA and applied it to the optimization of proton exchange membrane fuel cell (PEMFC) stack model parameters. The validity of the proposed method in determining the maximum output power and optimal operating state of the stack is verified through four cases [29]. With the help of the adaptive SSA, Liu and Rodriguez took a residential building as an example and took the energy load demand and investment cost as the optimization objectives to get the best combination scheme of the integrated sustainable energy systems, which achieved the purpose of reducing energy consumption and saving economic expenses [30].

LAA is known as the basic and one of the most practical geometric configurations of antenna array in which all elements are arranged in a straight line. Aimed at the design and optimization of LAA, a new modified SSA is proposed in this paper. The main contributions are briefly highlighted as follows:

(i) Proposition of the MSSA to further enhance the performance of SSA

(ii) Application of the algorithm to the electromagnetics and antenna community for the first time

(iii) Design of a few different scenarios of LAA for the maximum SLL reduction by optimizing the element spacing and excitation amplitude

(iv) Consideration of an additional constraint on the total length of the antenna array to preserve the features of the beam pattern

(v) Comparison of the results with several classical and well-known algorithms in function optimization and antenna array design problem

(vi) EM simulation with Altair FEKO 2019 to test the validity of the experiment results in practical conditions

The rest of this paper is structured as follows. Section 2 describes the basic principle of SSA, introduces the improvement strategies, and gives the pseudocode of the modified algorithm. Section 3 verifies its effectiveness and convergence performance. In Section 4, the mathematical description of the LAA optimization problem is given, and the simulation results are discussed and analyzed, and then, the EM verification experiment is carried out. Finally, Section 5 draws the conclusion of this paper.

2. The Sparrow Search Algorithm and Its Modification

2.1. Standard Sparrow Search Algorithm. A sparrow is an intelligent social animal, which keeps alert and stays a safe distance at all times. They also show great unity when encountering the enemy. According to their different behavior rules, sparrows can be divided into three roles: producers, scroungers, and scouters. Assuming that there are N sparrows in a D-dimensional search space, the position of the ith sparrow can be expressed as $X_i = [X_{i,1}, X_{i,2}, \cdots, X_{i,D}]$, $i = 1, 2, \cdots, N$. The following is an introduction of the three updating methods.

2.1.1. Producers. Producers are sparrows with better fitness values in the population. They have a wide search range and are responsible for searching and providing foraging directions for the whole population. The mathematical expression of producers is described as follows:

$$X_{i,j}^{t+1} = \begin{cases} X_{i,j}^{t} \cdot \exp\left(-\dfrac{i}{\alpha \cdot t_{\max}}\right), & R_2 < \mathrm{ST}, \\ X_{i,j}^{t} + Q \cdot L, & R_2 \geq \mathrm{ST}, \end{cases} \tag{1}$$

where t represents the current iteration number and $t_{\max}$ represents the maximum number of iterations. $X_{i,j}$ denotes the position of the ith sparrow in the jth dimension. α is a uniform random number in the range $(0, 1]$, and R_2 and ST represent the alarm value and the safety threshold respectively, where $R_2 \in [0, 1]$ and $\mathrm{ST} \in [0, 1]$. Q is a random number with normal distribution. L is a one-dimensional matrix with all elements of 1. When $R_2 < \mathrm{ST}$, it means that the surrounding environment is safe and they can search for food

extensively. When $R_2 \geqq \mathrm{ST}$, it means that there is danger at this time, and all sparrows have to fly to other safe areas quickly.

2.1.2. Scroungers. Scroungers are sparrows except all the producers and keep an eye on the producers. If they find that the producers have found better food, they will immediately leave their present position to fight for food and make themselves the producers. The position of the scroungers is updated as follows:

$$X_{i,j}^{t+1} = \begin{cases} Q \cdot \exp\left(\dfrac{X_{\text{worst}} - X_{i,j}^{t}}{i^2}\right), & i > \dfrac{N}{2}, \\ X_p^{t+1} + \left|X_{i,j}^{t} - X_P^{t+1}\right| \cdot A^{+} \cdot L, & i \leq \dfrac{N}{2}, \end{cases} \tag{2}$$

where X_{worst} represents the global worst position of the current population and X_p represents the best position occupied by the producers in the current iteration process. A is a one-dimensional matrix with elements of 1 or -1, and $A^{+} = (AA^{T})^{-1}$. If $i > N/2$, it indicates that the ith scrounger with low fitness value is in an unfavorable position and needs to expand his flight range to obtain food; if $i \leq N/2$, the ith scrounger will find a random place near the optimal location and perform local search.

2.1.3. Scouters. The scouters are randomly generated between the producers and the scroungers and can perceive whether there is danger in the foraging area. The model of scouters can be formulated as follows:

$$X_{i,j}^{t+1} = \begin{cases} X_{\text{best}}^{t} + \beta \cdot \left|X_{i,j}^{t} - X_{\text{best}}^{t}\right|, & F_i > F_g, \\ X_{i,j}^{t} + K \cdot \left(\dfrac{\left|X_{i,j}^{t} - X_{\text{worst}}^{t}\right|}{(F_i - F_w) + \varepsilon}\right), & F_i = F_g, \end{cases} \tag{3}$$

where X_{best} represents the global optimal position of the current population, and it is also the safest location. As a step size control parameter, β is a random number subject to standard normal distribution. $K \in [-1, 1]$ indicates the direction of movement of the sparrows. F_i, F_g, and F_w represent the fitness value of the ith sparrow, the global optimal, and the worst fitness value of the current population, respectively. ε is a minimal constant that avoids zero division error. $F_i > F_g$ indicates that the sparrow is at the edge of the population, vulnerable to predators, and needs to move to a safe area. $F_i = F_g$ indicates that the sparrow is in the middle of the population, but it is aware of the danger and needs to be close to other sparrows to reduce the risk of predation.

2.2. Modified Sparrow Search Algorithm. Compared with other representative intelligent optimization algorithms in recent years, although SSA has strong competitiveness in convergence speed, accuracy, and stability [31], it is still inevitable to fall into local optimum at the later stage of iterations, resulting in insufficient convergence accuracy [32]. In order to further improve the performance of the algorithm, this paper proposes a new modified algorithm based on chaotic adaptive inertia weight and improved boundary constraint.

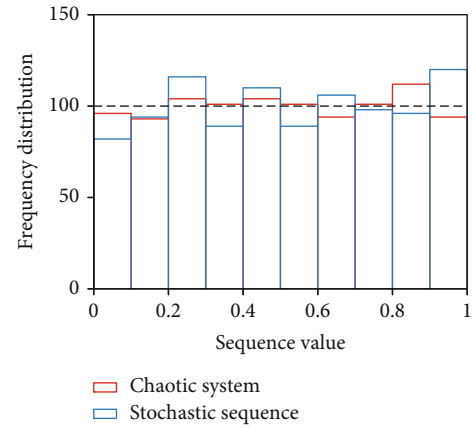

Figure 1: Statistical histogram of an ordinary random sequence and chaotic sequence.

2.2.1. Homogeneous Chaotic System. The quality of initial solution directly affects whether the algorithm can find the optimal solution. Chaos is a kind of random phenomenon with ergodicity, inherent regularity, and long-term unpredictability [33]. Within the search range of feasible solutions, chaotic sequences are widely used in population initialization of optimization algorithms; this is because they can traverse all states without repetition [34]. The research in Reference [35] shows that the homogeneous chaotic system has better random effect in variable initialization. Its function is expressed as

$$\begin{cases} \mu(t+1) = 3.5\mu(t)^2 + 3.3\mu(t) - 0.265, \\ \bar{X}(t+1) = \dfrac{1}{\pi} \arcsin\left(-\dfrac{7}{4}\mu(t+1) - \dfrac{33}{40}\right), \end{cases} \tag{4}$$

where $\mu \in [-73/70, 1/10]$ is the initialization sequence and $\bar{X}$ is completely chaotic in $[-1/2, 1/2]$. The formula for transforming chaotic sequence $\bar{X}$ into the solution space is as follows:

$$X = \frac{\mathrm{Ub} + \mathrm{Lb}}{2} + \bar{X}(\mathrm{Ub} - \mathrm{Lb}), \tag{5}$$

where Ub and Lb, respectively, represent the upper and lower boundary values of the optimized variables.

The statistical histogram obtained from the numerical statistics of ordinary random sequences and sequences generated by the homogeneous chaotic system is shown in Figure 1. It can be seen from the figure that the chaotic system has better homogenization, that is, better randomness. Hence, when the diversity of the sparrows increases, the quality of initial solution can be improved.

2.2.2. Adaptive Inertia Weight. All intelligent optimization algorithms include two processes of global exploration and local exploitation. An efficient algorithm needs to balance the global exploration capability and the local exploitation capability [36]. From the basic principle of SSA in Section 2.1, it is not difficult to find that the producer's search ability plays a vital role in whether the algorithm can find the optimal solution. Therefore, inertia weight w is introduced to adjust it adaptively. The mathematical expression is shown in

$$w = w_{\min} + (w_{\max} - w_{\min}) \cdot \text{rand}\,(1) \cdot \exp\left(-\frac{t}{t_{\max}}\right). \quad (6)$$

Take $w_{\max} = 0.1$ and $w_{\min} = 0.01$. The schematic diagram is illustrated in Figure 2.

As can be noticed, as the number of iterations increases, the inertia weight decreases adaptively. The update formula of the producers' position is modified as follows:

$$X_{i,j}^{t+1} = \begin{cases} X_{i,j}^{t} \cdot \exp\left(-\dfrac{i}{w \cdot \alpha \cdot t_{\max}}\right), & R_2 < \text{ST}, \\ X_{i,j}^{t} + Q \cdot L, & R_2 \geq \text{ST}. \end{cases} \quad (7)$$

By introducing the adaptive inertia weight, sparrow individuals can search favorable regions in the global range with a larger step size in the early stage of search and strengthen the ability of global exploration; in the later stage of the search, a smaller weight w can ensure sparrows to do fine search near the extreme points and strengthen the ability of local exploitation, so that the algorithm has a greater probability of converging to the global optimal value.

2.2.3. Improved Boundary Constraint. In the standard SSA, the processing strategy for sparrows overstepping the boundary is generally given by

$$X_{i,j}^{t+1} = \begin{cases} \text{Ub}, & X_{i,j}^{t+1} > \text{Ub}, \\ \text{Lb}, & X_{i,j}^{t+1} < \text{Lb}. \end{cases} \quad (8)$$

In this method, the individual that oversteps the boundary is simply assigned to the boundary value of the search range, which is equivalent to giving up the individual's search information. In the iterative process, if more individuals overstep the boundary, the positions of sparrows will accumulate more boundary values, resulting in the decrease in population diversity, which directly affects the convergence accuracy of the algorithm [37]. The strategy of improved boundary constraint handling is shown in Algorithm 1. Sparrows that overstep the boundary will randomly determine a position near the optimal position of the population, which enhances the diversity of the population and improves the global optimization ability of the algorithm to a certain extent.

The SSA modified by the above strategies is named MSSA, and the pseudocode outlining the steps of its implementation is shown in Algorithm 2.

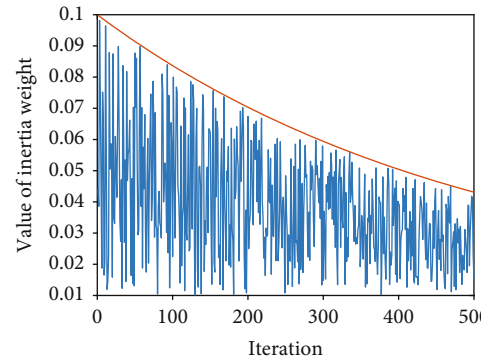

Figure 2: Schematic diagram of inertia weight.

3. Performance Analysis

In this section, MATLAB is used to verify and analyze the computational performance of MSSA on benchmark test functions. In order to verify the effectiveness and superiority of the modified algorithm, classical PSO and representative algorithms in recent years, including PSOGSA, WOA, GOA, and MTDE, are adopted for comparative experiments. All the parameters of these algorithms are in accordance with the original papers, as shown in Table 1.

The population size of all algorithms is set to 30, and the number of iterations is 500, for fairness. All numerical experiments are implemented on Intel(R) Core(TM) i5-9400U CPU with 2.90 GHz and 8 GB RAM.

3.1. Benchmark Test Functions. In order to comprehensively evaluate the global and local optimization ability of the algorithm, the experiment uses three types of benchmark test functions, in which the unimodal function has only a global optimal value but no local optimal value, so it can better test the local exploitation ability of the algorithm; the multimodal function has many local optimal values, so it can test the ability of the algorithm to jump out of the local extreme value and the global exploration ability. Table 2 shows the benchmark test functions for the experiment.

3.2. Experimental Results and Analysis. Considering the randomness of algorithm operation, 50 tests were run independently in order to make the results more convincing and universal. The best value and the worst value can show the exploration ability of the algorithm, and the mean value and standard deviation can show the accuracy and stability of the algorithm. Therefore, the best value, the worst value, and the mean value of 50 experimental results were statistically analyzed, and the standard deviation was calculated. The numerical results are shown in Table 3, where the optimal value is expressed in bold.

As can be seen from the results in Table 3, for unimodal functions F1~F3, the accuracy and stability of MSSA are greatly improved as compared to the other six algorithms, and the results of multiple optimizations can converge to the optimal value of the functions with the smallest standard deviation. For multimodal functions F4~F6, MSSA as well as SSA has excellent performance, and their ability to escape

Input: $X_{i,j}^{*}$ (Position that overstep the boundary), Ub (Upper boundary), Lb (Lower boundary), X_{best} (Global optimal position), X_{good} (Current optimal position)
Output: $X_{i,j}^{*}$ (The new position)

if $X_{i,j}^{*} < Lb \,||\, X\,i,j > Ub$ **then**
  $temp = X_{best} + |\, X_{best} - X_{good}\,| \cdot rand(1)$;
  if $Lb \le temp \le Ub$ **then**
    $X_{i,j}^{*} = temp$;
  else
    $X_{i,j}^{*} = X_{good}$;
  end if
end if
return $X_{i,j}^{*}$

Algorithm 1: Improved boundary constraint.

Input: N (Population size), D (Dimension size), P_{Num} (Producers size), S_{Num} (Scouters size), ST (Safety threshold), t (Initial iteration), t_{max} (Maximum iterations)
Output: X_{best} (Global optimal position), F_{best} (Fitness of global optimal position)

/∗Initializing∗/
Randomly generate the positions of N sparrows $X_{i,j}$ by homogeneous chaotic system (i=1,2,…,N, j=1,2,…,D);
Calculate the fitness of each sparrow F_i;
Find X_{best} and F_{best};
/∗Iterating∗/
while $t < t_{max}$ **do**
  Sort the F_i and find global worst position X_{worst};
  $R_2 = rand(1)$;
  for $i = 1 : P_{Num}$
    Evaluate and calculate the adaptive weight w;
    Update the position $X_{i,j}$ by (7);
    Check and adjust position that overstep the boundary by Algorithm 1;
  end for
  Sort the F_i and find the best position of producers X_p;
  for $i = (P_{Num} + 1) : N$
    Update the position $X_{i,j}$ by (2);
    Check and adjust position that overstep the boundary by Algorithm 1;
  end for
  for $i = 1 : S_{Num}$
    Update the position $X_{i,j}$ by (3);
    Check and adjust position that overstep the boundary by Algorithm 1;
  end for
    Evaluate and update X_{best} and F_{best};
    $t = t + 1$;
end while
return X_{best} and F_{best};

Algorithm 2: Modified sparrow search algorithm.

local optimal solutions and robustness are obviously better than those of the remaining algorithms. For fixed-dimensional multimodal functions F7~F9, all algorithms can find the optimal value of the functions. MSSA's performance is inferior to that of MTDE for function F7, but better than that of PSOGSA, GOA, and SSA. For function F8, the standard deviation of MSSA is the smallest, and MSSA performs best for function F9.

In order to directly reflect the convergence characteristics of the modified algorithm on the benchmark test functions, the average convergence curves of the seven algorithms are presented in Figure 3. The logarithmic axis is adopted for the y-axis to make data fluctuation much clearer. It can be seen from Figure 3 that MSSA not only has higher calculation accuracy but also significantly improves the convergence speed.

Table 1: Parameters of different algorithms.

Algorithm	Parameter	Value
PSO [38, 39]	Individual learning factor $c1$	2
	Social learning factor c_2	2
	Inertia weight w	1.05
PSOGSA [40]	Individual learning factor c_1	0.5
	Social learning factor c_2	1.5
	Weighting function w	$[0, 1]$
	Gravitational constant G	1
	Alpha α	20
WOA [41]	Variable a	$2 \longrightarrow 0$
	Constant defining logarithmic spiral shape b	1
GOA [42]	Minimum reduction factor $c_{\min}$	0.00004
	Maximum reduction factor $c_{\max}$	1
	Attraction intensity f	0.5
	Attractive length scale l	1.5
MTDE [43]	Number of portions divided by iterations WinIter	20
	Gbest-history size H	5
	Nonlinear decreased coefficient a_2	$0.001 \longrightarrow 2$
	Dimension-dependent value Mu	$\log(D)$
	Mean value of improved scale factors μ_f	0.5
	Variance of improved scale factors σ	0.2
SSA [23]	Number of producers P_{Num}	20%
	Number of scouters S_{Num}	10%
	Safety threshold ST	0.8

Aimed at observing the search process more intuitively, Figure 4 shows the search trajectories of sparrows on the three types of benchmark test functions of the MSSA. It can be seen that in the early iterations, sparrows are scattered over a large search space. As the number of iterations increases, the adaptive weight factor improves the local optimization ability of the algorithm, and precocity is avoided in the end. Consequently, most sparrows are able to gather in the optimal solution and its nearby area (red box in Figure 4).

3.3. Comparison of the Improved Factors. Tests are conducted to observe the performance of the three introduced improved factors. The standard SSA with the modifications of the homogeneous chaotic system function and the improved boundary constraint is named CSSA, while the SSA with the modifications of adaptive inertia weight and the improved boundary constraint is named ASSA. Figure 5 shows the convergence curves of the improved factors on the three types of benchmark test functions. It can be found from the figure that MSSA has better performance by combining those improved factors. The reason may be attributed to the fact that the adaptive inertia weight can speed up the local convergence rate. Chaos initialization and the improved boundary constraint can increase the diversity of population to a certain extent, which lays a good foundation for the improvement of the convergence accuracy.

3.4. Statistical Testing. The Wilcoxon rank sum test is performed to statistically identify significant differences between the two algorithms. The best values, worst values, mean values, and standard deviations of all benchmark test functions in Table 3 are adopted as test samples. A nonparametric test is done by comparing MSSA with PSO, PSOGSA, WOA, GOA, MTDE, and SSA respectively. It is generally considered that the algorithm is significantly different from others if the p value is less than 0.05. The results from Table 4 show that all the p values are less than 0.05, except for the result of MSSA versus SSA. This indicates that there are significant differences between MSSA and most algorithms at the 5% significance level. In the calculation of the above benchmark test functions, although the performance of MSSA is better than that of SSA, there is no significant difference between them.

3.5. Algorithm Complexity. The computational cost of the intelligent optimization algorithm is mainly determined by the evaluation of fitness function. Assuming that the maximum iteration is T, the complexity of MSSA can be written as $O(NT)$ since there is only one inner loop in the algorithm, where N is the population size. It can be seen that the computational complexity is linear with N and T. According to the above modifications, MSSA does not change the algorithm framework of SSA, so they have the same complexity, and the proposed algorithm does not reduce the solution efficiency.

3.6. Analysis of Asymptotic Property. For the minimization optimization problem, the fitness asymptotic property of MSSA is analyzed in this section. Suppose that the finite nonempty set $\mathbf{S}$ is the solution space and the optimal solution set $\Omega = \{x^* | x^* \in \mathbf{S}, f(x^*) < \varepsilon\}$, where f is the objective function and ε is the acceptable objective function value. Let the optimal sparrow position obtained by the algorithm in the tth iteration be x_t^*, and $\{d_t | d_t = f(x_t^*) - f(x^*),\ 1 \le t \le T\}$ is the nonnegative random process generated by the algorithm. Since the algorithm gets the optimal sparrow individual through the idea of survival of the fittest; hence, $P(f(x_{t+1}^*) - f(x_t^*) > 0) = 0$. In addition, because the sparrow population updates its position in three ways randomly, when $f(x_t^*) > f(x^*)$, $P(f(x_{t+1}^*) = f(x_t^*)) \neq 1$. Therefore, $P(f(x_{t+1}^*) - f(x_t^*) < 0) > 0$. Let $E[f(x_{t+1}^*) - f(x_t^*)] = -\tau_{t+1}$, and $\tau_{t+1} > 0$ can be obtained from the above analysis. Hence,

$$\begin{aligned} E[d_{t+1} - d_t] &= E[(f(x_{t+1}^*) - f(x_t^*)) - (f(x_t^*) - f(x^*))] \\ &= E[f(x_{t+1}^*) - f(x_t^*)] = -\tau_{t+1}. \end{aligned} \tag{9}$$

That is, $E(d_{t+1}) = E(d_t) - \tau_{t+1}$.

Let $\tau = \min\{\tau_1, \tau_2, \cdots, \tau_T\}$, and there is $E(d_{t+1}) \le E(d_t) - \tau$. Therefore, the fitness asymptotic property of MSSA can be proven, which means that the algorithm asymptotically converges to the optimal solution.

Table 2: Benchmark test functions.

Function's type	Function's name	Function's equation	D	Search space
Unimodal	Sphere	$F_1(x) = \sum_{i=1}^{D} x_i^2$	30	$[-100,100]$
	Schwefel 2.22	$F_2(x) = \sum_{i=1}^{D} \lvert x_i \rvert + \prod_{i=1}^{D} \lvert x_i \rvert$	30	$[-10, 10]$
	Schwefel 1.2	$F_3(x) = \sum_{i=1}^{D} \left(\sum_{j=1}^{i} x_j \right)^2$	30	$[-100,100]$
Multimodal	Rastrigin	$F_4(x) = \sum_{i=1}^{D} \left[x_i^2 - 10 \cos(2\pi x_i) + 10 \right]$	30	$[-5.12,5.12]$
	Ackley	$F_5(x) = -20 \exp\left(-0.2 \sqrt{\frac{1}{D} \sum_{i=1}^{D} x_i^2} \right) - \exp\left(\frac{1}{D} \sum_{i=1}^{D} \cos(2\pi x_i) \right) + 20 + e$	30	$[-32, 32]$
	Griewank	$F_6(x) = \frac{1}{4000} \sum_{i=1}^{D} x_i^2 - \prod_{i=1}^{D} \cos\left(\frac{x_i}{\sqrt{i}} \right) + 1$	30	$[-600,600]$
Fixed-dimension multimodal	Goldstein–Price	$F_7(x) = \left[1 + (x_1 + x_2 + 1)^2 \left(19 - 14x_1 + 3x_1^2 - 14x_2 + 6x_1x_2 + 3x_2^2 \right) \right] \times \left[30 + (2x_1 - 3x_2)^2 \times \left(18 - 32x_1 + 12x_1^2 + 48x_2 - 36x_1x_2 + 27x_2^2 \right) \right]$	2	$[-2, 2]$
	Hartman	$F_8(x) = -\sum_{i=1}^{4} c_i \exp\left(-\sum_{j=1}^{3} a_{ij} \left(x_j - p_{ij} \right)^2 \right)$	3	$[0, 1]$
	Shekel's foxholes	$F_9(x) = -\sum_{i=1}^{5} \left[(X - a_i)(X - a_i)^{\mathrm{T}} + c_i \right]^{-1}$	4	$[0, 10]$

Table 3: Numerical results.

	Value	PSO	PSOGSA	WOA	GOA	MTDE	SSA	MSSA
F1	Best	5.03e + 03	3.52e − 01	4.42e − 86	6.16e + 00	6.26e − 03	**0.00e + 00**	**0.00e + 00**
	Worst	9.04e + 03	1.00e + 04	1.18e − 68	1.31e + 02	7.22e − 01	2.60e − 69	**0.00e + 00**
	Mean	7.29e + 03	1.43e + 03	2.37e − 70	3.74e + 01	1.06e − 01	5.40e − 71	**0.00e + 00**
	Std	9.60e + 02	3.49e + 03	1.66e − 69	2.64e + 01	1.31e − 01	3.68e − 70	**0.00e + 00**
F2	Best	3.40e + 01	1.87e − 08	7.17e − 57	3.82e + 00	2.76e − 03	**0.00e + 00**	**0.00e + 00**
	Worst	5.83e + 01	8.13e + 01	2.93e − 49	8.62e + 01	3.09e − 01	1.40e − 34	**0.00e + 00**
	Mean	4.31e + 01	1.21e + 01	1.05e − 50	1.41e + 01	4.53e − 02	2.89e − 36	**0.00e + 00**
	Std	5.73e + 00	1.84e + 01	4.75e − 50	1.34e + 01	5.18e − 02	1.98e − 35	**0.00e + 00**
F3	Best	1.09e + 04	2.94e + 03	7.41e + 03	7.58e + 02	1.06e + 02	**0.00e + 00**	**0.00e + 00**
	Worst	3.34e + 04	5.34e + 04	8.57e + 04	7.27e + 03	1.07e + 03	2.38e − 51	**0.00e + 00**
	Mean	1.91e + 04	1.48e + 04	4.30e + 04	2.87e + 03	3.89e + 02	4.76e − 53	**0.00e + 00**
	Std	4.80e + 03	8.81e + 03	1.64e + 04	1.39e + 03	2.10e + 02	3.37e − 52	**0.00e + 00**
F4	Best	2.11e + 02	7.26e + 01	**0.00e + 00**	4.14e + 01	1.37e + 01	**0.00e + 00**	**0.00e + 00**
	Worst	2.70e + 02	2.32e + 02	1.13e − 13	1.76e + 02	4.41e + 01	**0.00e + 00**	**0.00e + 00**
	Mean	2.40e + 02	1.37e + 02	3.41e − 15	9.61e + 01	2.52e + 01	**0.00e + 00**	**0.00e + 00**
	Std	1.30e + 01	3.39e + 01	1.76e − 14	2.80e + 01	7.14e + 00	**0.00e + 00**	**0.00e + 00**
F5	Best	1.28e + 01	7.04e + 00	**8.88e − 16**	2.99e + 00	5.54e − 02	**8.88e − 16**	**8.88e − 16**
	Worst	1.51e + 01	1.92e + 01	7.99e − 15	8.99e + 00	2.50e + 00	**8.88e − 16**	**8.88e − 16**
	Mean	1.43e + 01	1.57e + 01	4.79e − 15	5.33e + 00	1.44e + 00	**8.88e − 16**	**8.88e − 16**
	Std	4.52e − 01	3.36e + 00	2.48e − 15	1.38e + 00	5.53e − 01	**0.00e + 00**	**0.00e + 00**
F6	Best	4.47e + 01	5.66e − 01	0.00e + 00	8.69e − 01	2.26e − 02	**0.00e + 00**	**0.00e + 00**
	Worst	8.84e + 01	9.19e + 01	1.60e − 01	1.40e + 00	6.12e − 01	**0.00e + 00**	**0.00e + 00**
	Mean	6.65e + 01	2.13e + 01	7.85e − 03	1.11e + 00	1.27e − 01	**0.00e + 00**	**0.00e + 00**
	Std	8.99e + 00	3.74e + 01	3.26e − 02	1.01e − 01	1.15e − 01	**0.00e + 00**	**0.00e + 00**
F7	Best	**3.00e + 00**	**3.00e + 00**	**3.00e + 00**	**3.00e + 00**	**3.00e + 00**	**3.00e + 00**	**3.00e + 00**
	Worst	3.05e + 00	8.40e + 01	**3.00e + 00**	8.40e + 01	**3.00e + 00**	3.00e + 01	3.00e + 01
	Mean	3.01e + 00	6.24e + 00	3.54e + 00	7.86e + 00	**3.00e + 00**	5.16e + 00	4.62e + 00
	Std	8.78e − 03	1.60e + 01	3.78e + 00	1.92e + 01	**2.29e − 15**	7.32e + 00	6.48e + 00
F8	Best	**−3.86e + 0**	**−3.86e + 0**	**−3.86e + 0**	**−3.86e + 0**	**−3.86e + 0**	**−3.86e + 0**	**−3.86e + 0**
	Worst	−3.85e + 0	**−3.86e + 0**	−3.09e + 0	−3.03e + 0	**−3.86e + 0**	−3.08e + 0	**−3.86e + 0**
	Mean	**−3.86e + 0**	**−3.86e + 0**	−3.83e + 0	−3.73e + 0	**−3.86e + 0**	−3.85e + 0	**−3.86e + 0**
	Std	1.52e − 03	2.90e − 15	1.09e − 01	2.53e − 01	3.13e − 15	1.08e − 01	**2.83e − 15**
F9	Best	−9.51e + 0	**−1.02e + 1**	**−1.02e + 1**	**−1.02e + 1**	**−1.02e + 1**	**−1.02e + 1**	**−1.02e + 1**
	Worst	−2.14e + 0	−2.63e + 0	−2.63e + 0	−2.63e + 0	**−5.06e + 0**	**−5.06e + 0**	**−5.06e + 0**
	Mean	−6.31e + 0	−6.58e + 0	−7.49e + 0	−6.44e + 0	−9.23e + 0	−8.62e + 0	**−9.54e + 0**
	Std	2.32e + 00	3.32e + 00	3.04e + 00	3.29e + 00	1.98e + 00	2.33e + 00	**1.67e + 00**

4. Experiments on Maximum SLL Reduction of LAA

In order to test the feasibility of optimizing EM problems based on the MSSA, this section designed the simulation experiments of optimizing the element spacings and excitation amplitudes of LAA through MATLAB. Firstly, the system model is presented and the fitness function is formulated. Secondly, different design scenarios of maximum SLL reduction are simulated by MSSA, and the obtained results are compared with those of PSO, PSOGSA, WOA, GOA, MTDE, and SSA. Then, the stability of the algorithms is

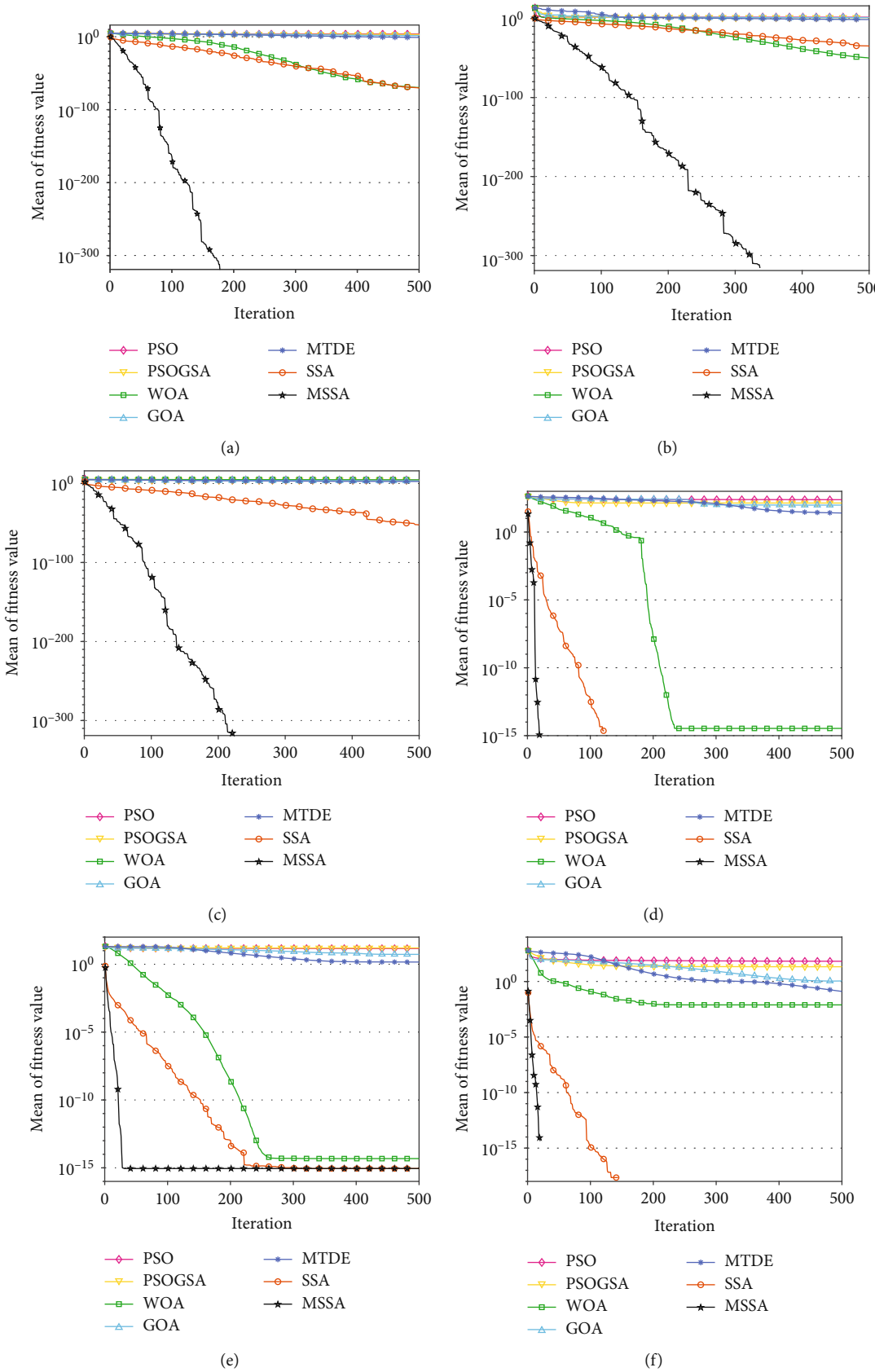

Figure 3: Continued.

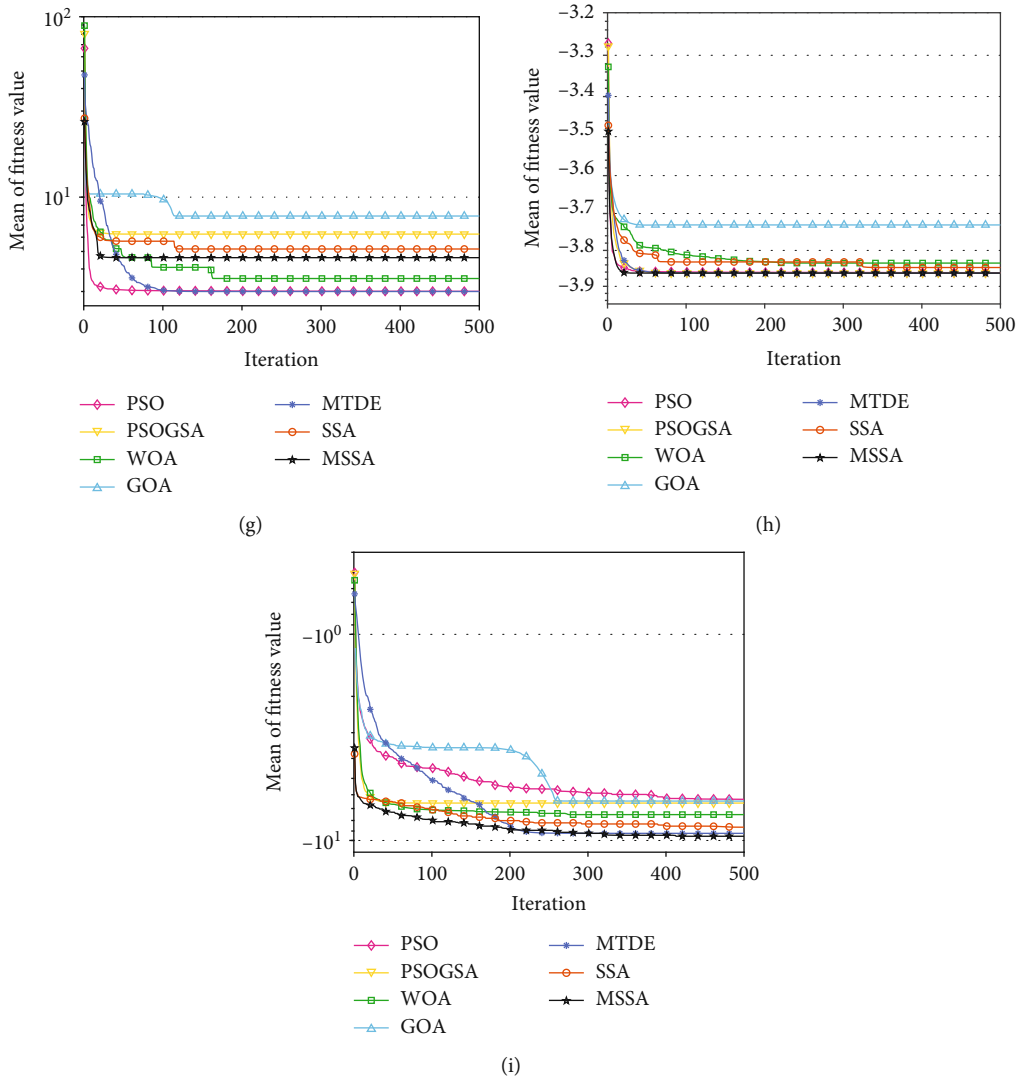

FIGURE 3: Convergence curves of the 7 algorithms on the benchmark test functions: (a) F1; (b) F2; (c) F3; (d) F4; (e) F5; (f) F6; (g) F7; (h) F8; (i) F9.

analyzed. Finally, the optimization performance is verified by FEKO EM simulation under practical conditions.

4.1. Problem Formulation. Considering the symmetry of $2N$ isotropic element LAA in Figure 6, the array factor can be expressed as follows:

$$\mathrm{AF}(\varphi) = 2\sum_{n=1}^{N} I_n \cos\left(kx_n \cos\left(\varphi\right) + \psi_n\right), \tag{10}$$

where $k = 2\pi/\lambda$ is the wave number and I_n, x_n, and ψ_n, respectively, represent the excitation amplitude, position, and phase of the nth element. φ symbolizes the azimuth angle, which is defined as the angle with the positive x-axis.

In this paper, the element spacing and excitation amplitude are taken as optimization variables, and the optimization objective is to suppress the maximum SLL. Therefore, the fitness function can be formulated as

$$\min \ \text{fitness} = \max\left\{20\log_{10}\frac{|\mathrm{AF}(\varphi_{\mathrm{SL}})|}{|\mathrm{AF}(\varphi_{\mathrm{ML}})|}\right\}, \tag{11}$$

$$\text{s.t.} \quad \varphi_{\mathrm{ML}} = \arg\max|\mathrm{AF}(\varphi)|, \quad \varphi \in [0,\pi], \tag{12}$$

$$\varphi_{\mathrm{SL}} \in [0,\varphi_{\mathrm{FN1}}] \cup [\varphi_{\mathrm{FN2}},\pi], \tag{13}$$

$$0 < d_i < \lambda, \quad \forall i \in N, \tag{14}$$

$$0 < I_i < 1, \quad \forall i \in N, \tag{15}$$

where φ_{SL} and φ_{ML} represent the region of the side lobe and main lobe, respectively. φ_{FN1} and φ_{FN2} are the first nulls of the pattern. Constraints (14) and (15) define the range in optimizing the element spacing and excitation amplitude. Based on the HF vertical antenna array, the number of elements is chosen as 8, 16, and 24 to test the optimization ability of the algorithm in different dimensions. In order to maintain

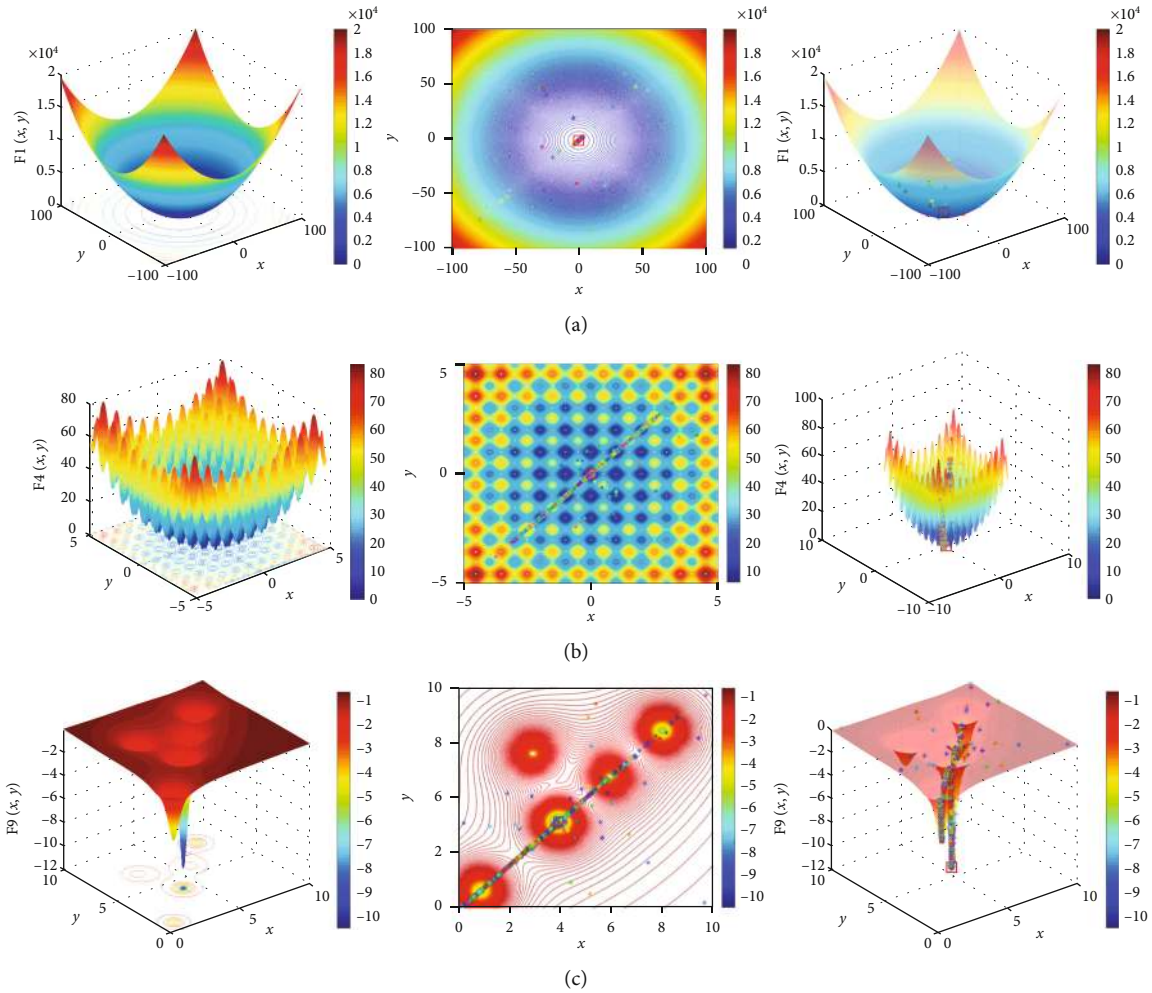

FIGURE 4: Iterative trajectories of MSSA on the benchmark test functions: (a) unimodal F1; (b) multimodal F4; (c) fixed-dimension multimodal F9.

the first null beam width to the maximum extent, for LAA with $2N$ of 8, 16, and 24, φ_{FN1} is limited to 75°, 82°, and 85° and φ_{FN2} is 105°, 98°, and 95°, respectively.

4.2. Experiments on Maximum SLL Reduction with Optimized Element Spacing. In this section, seven algorithms are used to optimize the positions of 8-element, 16-element, and 24-element LAA, respectively. Because the median is not affected by small or large data, it can better reflect the average optimization ability of the algorithms. Therefore, the median value of 25 independent repeated experiments is presented.

4.2.1. 8-Element LAA. Since this is a symmetric array, the spatial dimension of solution is 4. Figure 7 shows the 3D radiation patterns of 8-element LAA before and after MSSA optimization. It can be seen intuitively from the figure that MSSA can effectively reduce the maximum SLL.

Figure 8(a) shows the beam patterns obtained by different algorithms, and Figure 8(b) shows the convergence curves of different algorithms, in which conventional LAA refers to the unoptimized LAA while maintaining uniform element position distribution and uniform excitation amplitude. It can be seen from the figure that the convergence speed and convergence accuracy of MSSA have been improved. The maximum SLL optimized by different algorithms for 8-element LAA is shown in Table 5. As shown, the maximum SLL obtained by MSSA is -20.2186 dB, which is the lowermost among all algorithms. There is an improvement of 7.4214 dB using the proposed approach as compared to the conventional technique. Table 5 also gives the optimized positions of the elements obtained by different algorithms.

4.2.2. 16-Element LAA. In order to maintain the main lobe shape and beam width, it is necessary to impose additional constraint on the total length of the antenna array, as shown in the following formula:

$$\begin{cases} x_1 = 0.25\lambda, \\ x_N = \dfrac{(2N-1)d}{2}. \end{cases} \tag{16}$$

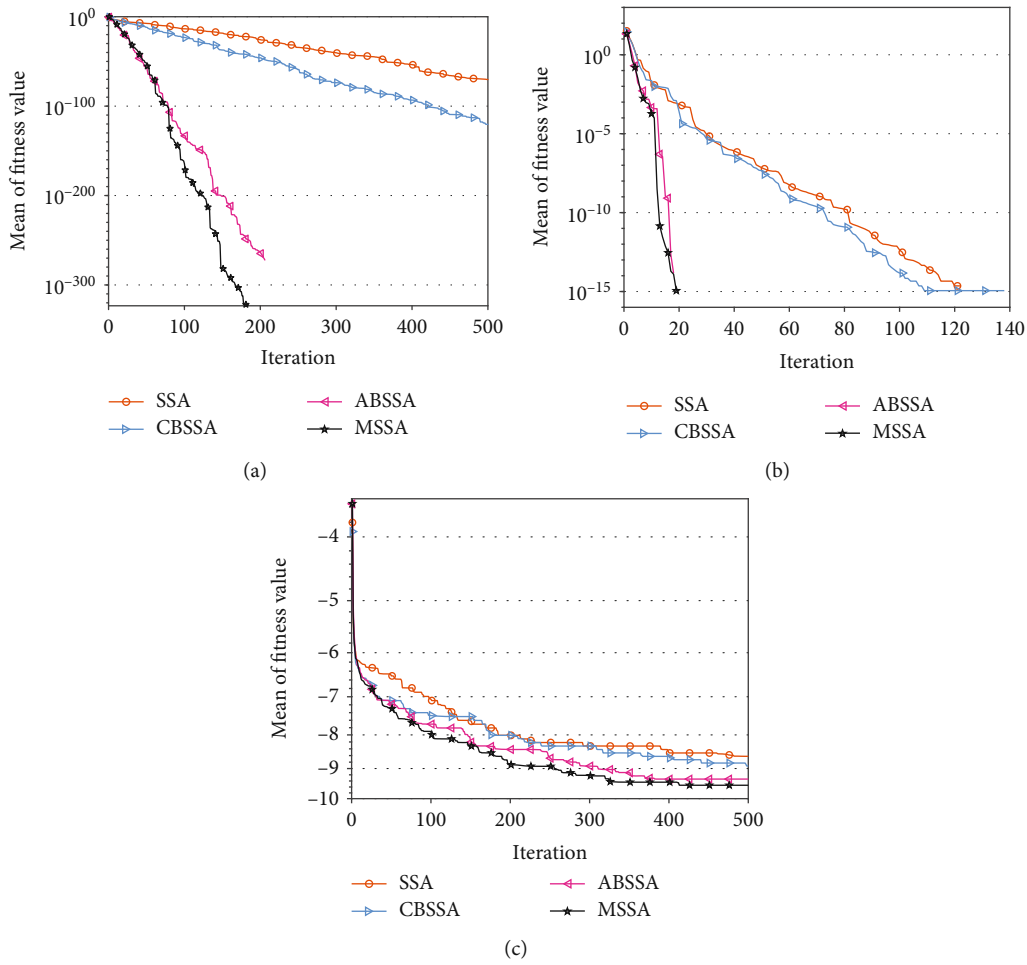

Figure 5: Convergence curves of the improved factors on the benchmark test functions: (a) unimodal F1; (b) multimodal F4; (c) fixed-dimension multimodal F9.

Table 4: p value of the nonparametric test between MSSA and other algorithms.

	PSO	PSOGSA	WOA	GOA	MTDE	SSA
p value	$1.57e-06$	$2.20e-06$	$1.90e-03$	$4.54e-06$	$9.32e-05$	$2.38e-01$

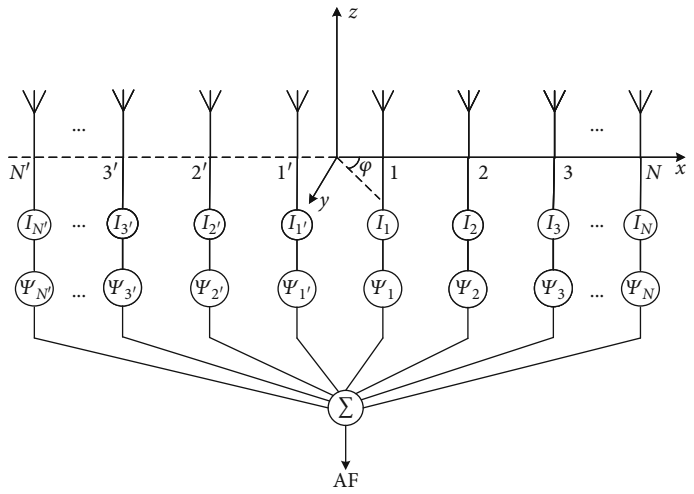

Figure 6: Geometric distribution of $2N$-element LAA.

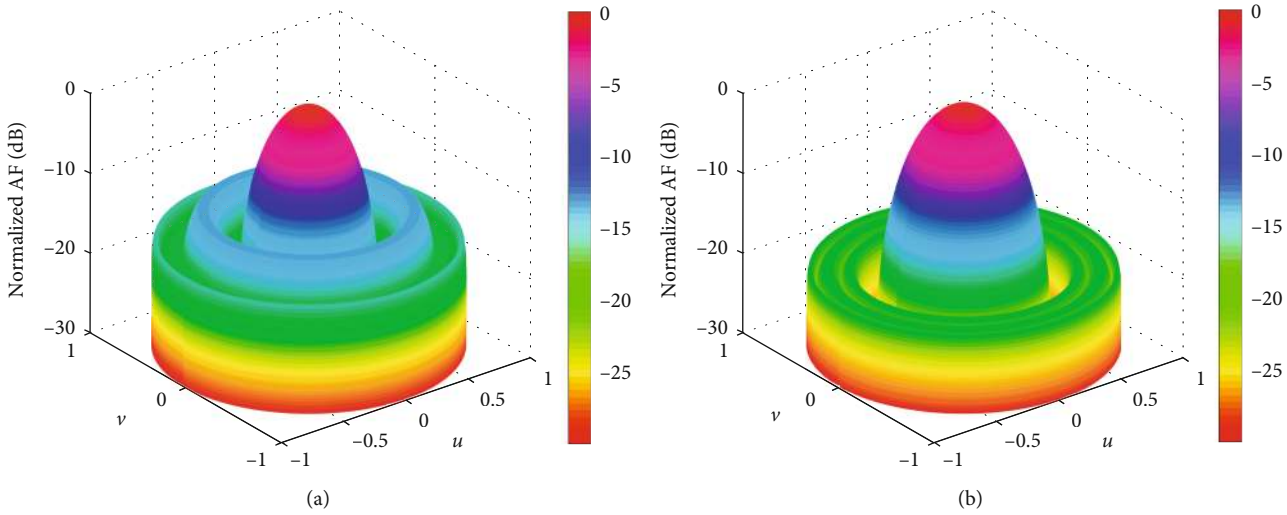

Figure 7: 3D radiation patterns of 8-element LAA before and after MSSA optimization: (a) before optimization; (b) after optimization.

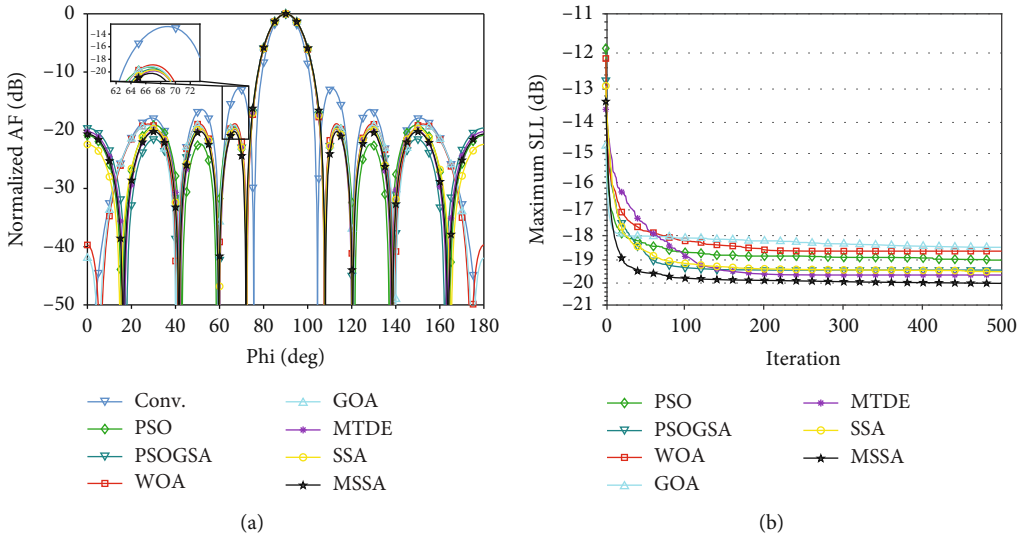

Figure 8: Beam patterns and convergence curves of 8-element LAA optimized by different algorithms: (a) beam patterns; (b) convergence curves.

Table 5: Optimized element positions and maximum SLL of 8-element LAA by different algorithms.

Algorithm	Optimized element positions (λ)	Maximum SLL (dB)
Conv.	0.2500, 0.7500, 1.2500, 1.7500	-12.7972
PSO	0.1243, 0.6381, 0.9773, 1.6283	-19.1209
PSOGSA	0.1120, 0.6269, 1.0036, 1.6384	-19.5447
WOA	0.1625, 0.6044, 1.0286, 1.6326	-18.8768
GOA	0.1529, 0.6016, 1.0115, 1.6185	-19.1405
MTDE	0.1274, 0.6228, 1.0082, 1.6497	-19.8331
SSA	0.1340, 0.6179, 1.0087, 1.6427	-19.6800
MSSA	0.1067, 0.6216, 0.9832, 1.6298	-20.2186

The spacing between the first two elements on both sides of the y-axis is fixed at 0.5λ, so as to ensure that one antenna pair in the antenna array meets Nyquist spatial sampling. The Nth element is fixed at $x_n = (2N-1)d/2$, where $d = 0.5\lambda$ represents the default spacing of the uniform LAA, thereby suppressing the distortion of the main lobe [44]. Since the positions of the first and last elements on both sides of the antenna array are fixed, the positions of other elements are variable. Therefore, the optimized dimension is simplified to $2N-2$.

Figure 9 depicts 3D radiation patterns of 16-element LAA before and after optimization by MSSA. Figure 10 depicts the beam patterns and convergence curves of 16-element LAA optimized by different algorithms. It can be seen that MSSA outperforms other algorithms. Both the positions of 16-element LAA optimized by different algorithms and corresponding maximum SLL are listed in

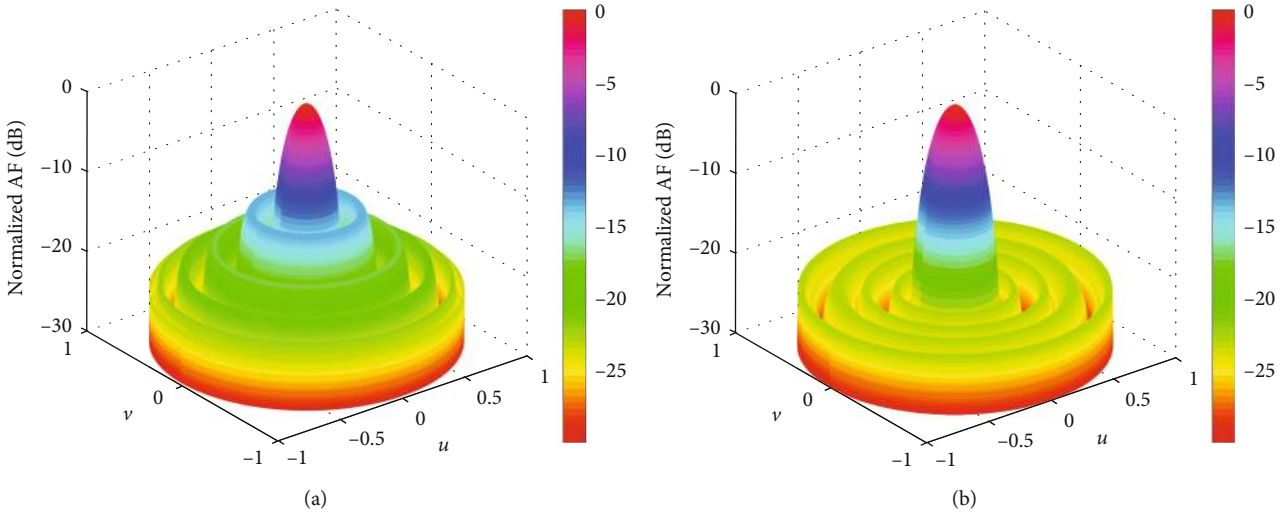

Figure 9: 3D radiation patterns of 16-element LAA before and after MSSA optimization: (a) before optimization; (b) after optimization.

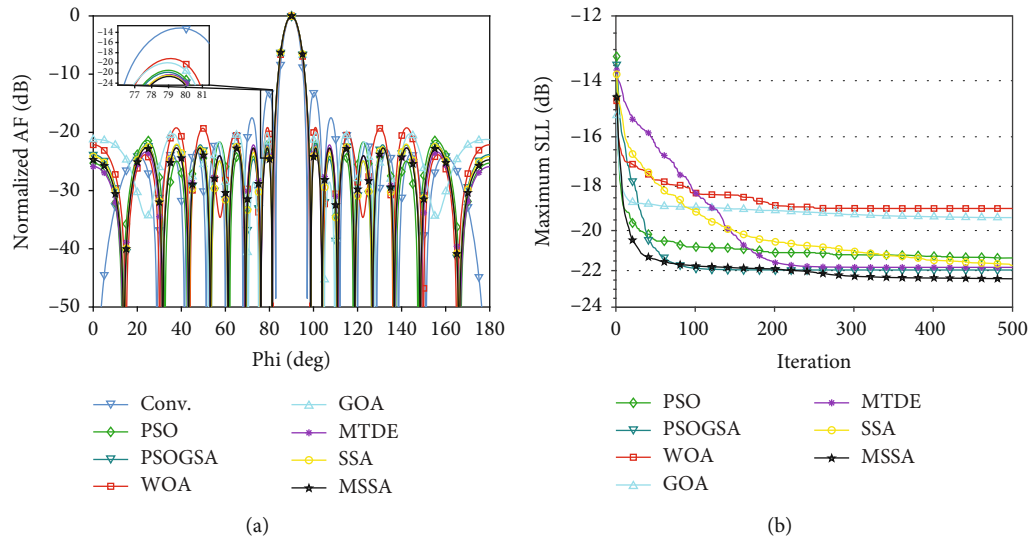

Figure 10: Beam patterns and convergence curves of 16-element LAA optimized by different algorithms: (a) beam pattern; (b) convergence curves.

Table 6. The maximum SLL obtained by MSSA is 9.5292 dB lower than that of the conventional array.

4.2.3. 24-Element LAA. The position constraints of the 24-element LAA are the same as above; that is, the first element is fixed at 0.25λ and the 12th element is fixed at 5.75λ. Therefore, the spatial dimension of solution is simplified to 10.

The 3D radiation patterns of 24-element LAA before and after MSSA optimization are given in Figure 11. Figure 12 shows the beam patterns and convergence curves obtained by different algorithms. Table 7 displays the optimized results and the maximum SLL of 24-element LAA with different algorithms simultaneously. Compared with the conventional method, PSO, PSOGSA, WOA, GOA, MTDE, and SSA, MSSA has better optimization effect, and the maximum SLL is reduced by 10.8158 dB, 3.1391 dB, 1.2248 dB, 6.2655 dB, 5.0487 dB, 0.7132 dB, and 0.8840 dB, respectively.

4.3. Experiments on Maximum SLL Reduction with Optimized Excitation Amplitude. This section conducts and analyzes the optimization performance of MSSA on LAA excitation amplitude. Corresponding to the previous section, different algorithms are used to optimize the 8-element, 16-element, and 24-element LAA.

4.3.1. 8-Element LAA. It can be seen from the 3D radiation patterns of the antenna array in Figure 13 that the maximum SLL of the optimized LAA is significantly reduced. Figure 14 shows the beam patterns and convergence curves of different algorithms. The element excitation amplitude is normalized, and the obtained amplitude is the largest at the center of

Table 6: Optimized element positions and maximum SLL of 16-element LAA by different algorithms.

Algorithm	Optimized element positions (λ)	Maximum SLL (dB)
Conv.	0.2500, 0.7500, 1.2500, 1.7500, 2.2500, 2.7500, 3.2500, 3.7500	-13.1476
PSO	0.2500, 0.5311, 1.0128, 1.3930, 1.8738, 2.3329, 2.9893, 3.7500	-21.3693
PSOGSA	0.2500, 0.5495, 1.0230, 1.3560, 1.8561, 2.3358, 2.9783, 3.7500	-21.8484
WOA	0.2500, 0.6485, 1.0456, 1.3751, 1.9467, 2.4634, 3.0076, 3.7500	-19.1546
GOA	0.2500, 0.5802, 1.1274, 1.3493, 1.9119, 2.3129, 3.0208, 3.7500	-19.9808
MTDE	0.2500, 0.5244, 1.0082, 1.3555, 1.8647, 2.3620, 3.0093, 3.7500	-22.1498
SSA	0.2500, 0.5331, 1.0118, 1.3453, 1.8495, 2.3404, 2.9835, 3.7500	-22.0177
MSSA	0.2500, 0.5226, 1.0038, 1.3486, 1.8518, 2.3447, 2.9948, 3.7500	-22.6768

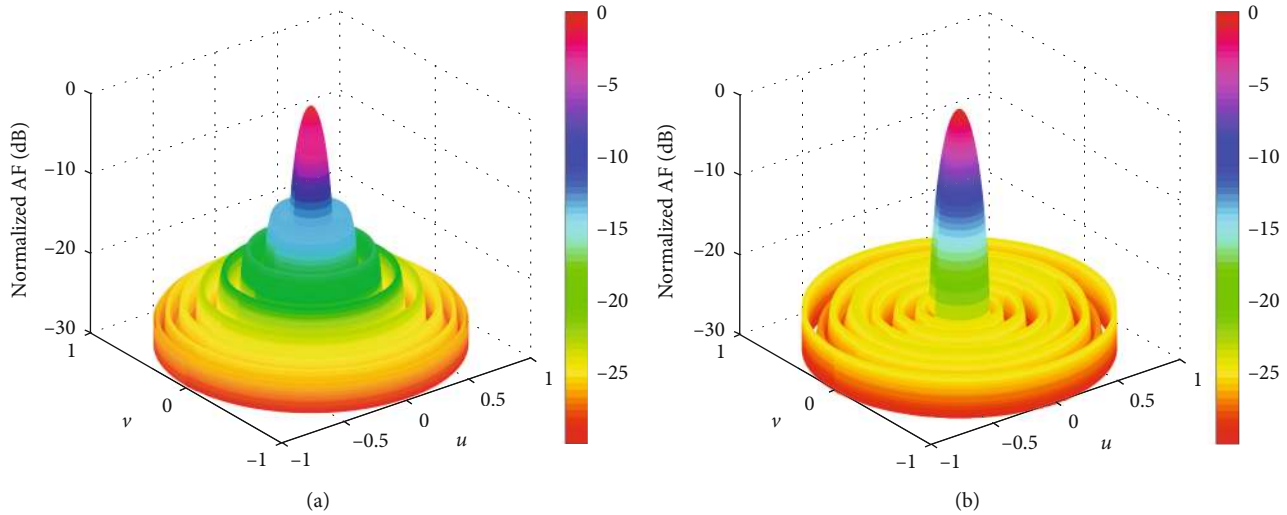

Figure 11: 3D radiation patterns of 24-element LAA before and after MSSA optimization: (a) before optimization; (b) after optimization.

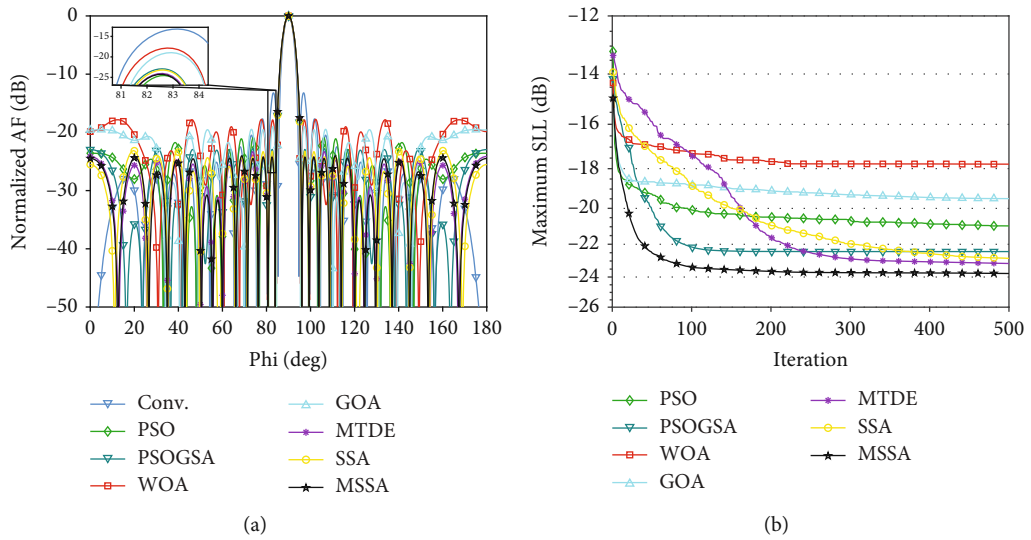

Figure 12: Beam patterns and convergence curves of 24-element LAA optimized by different algorithms: (a) beam patterns; (b) convergence curves.

Table 7: Optimized element positions and maximum SLL of 24-element LAA by different algorithms.

Algorithm	Optimized element positions (λ)	Maximum SLL (dB)
Conv.	0.2500, 0.7500, 1.2500, 1.7500, 2.2500, 2.7500, 3.2500, 3.7500, 4.2500, 4.7500, 5.2500, 5.7500	-13.2091
PSO	0.2500, 0.5328, 0.9972, 1.2560, 1.7894, 2.1072, 2.5783, 3.0281, 3.5374, 4.2919, 5.0668, 5.7500	-20.8858
PSOGSA	0.2500, 0.4890, 1.0882, 1.2757, 1.7539, 2.0904, 2.6058, 3.1024, 3.5855, 4.2269, 4.9847, 5.7500	-22.8001
WOA	0.2500, 0.4275, 1.0262, 1.3683, 1.7913, 2.4037, 3.1937, 3.2078, 3.9114, 4.2607, 5.0305, 5.7500	-17.7594
GOA	0.2500, 0.6940, 1.1051, 1.2948, 1.8599, 2.3254, 2.8115, 3.2905, 3.9984, 4.4875, 5.1074, 5.7500	-18.9762
MTDE	0.2500, 0.5035, 0.9885, 1.2737, 1.7304, 2.1064, 2.5789, 3.0315, 3.5594, 4.2334, 4.9549, 5.7500	-23.3117
SSA	0.2500, 0.5314, 0.9701, 1.2658, 1.7411, 2.1524, 2.6184, 3.0450, 3.5985, 4.2726, 4.9465, 5.7500	-23.1409
MSSA	0.2500, 0.4950, 0.9690, 1.2760, 1.7106, 2.1075, 2.5880, 3.0307, 3.5357, 4.2088, 4.9494, 5.7500	-24.0249

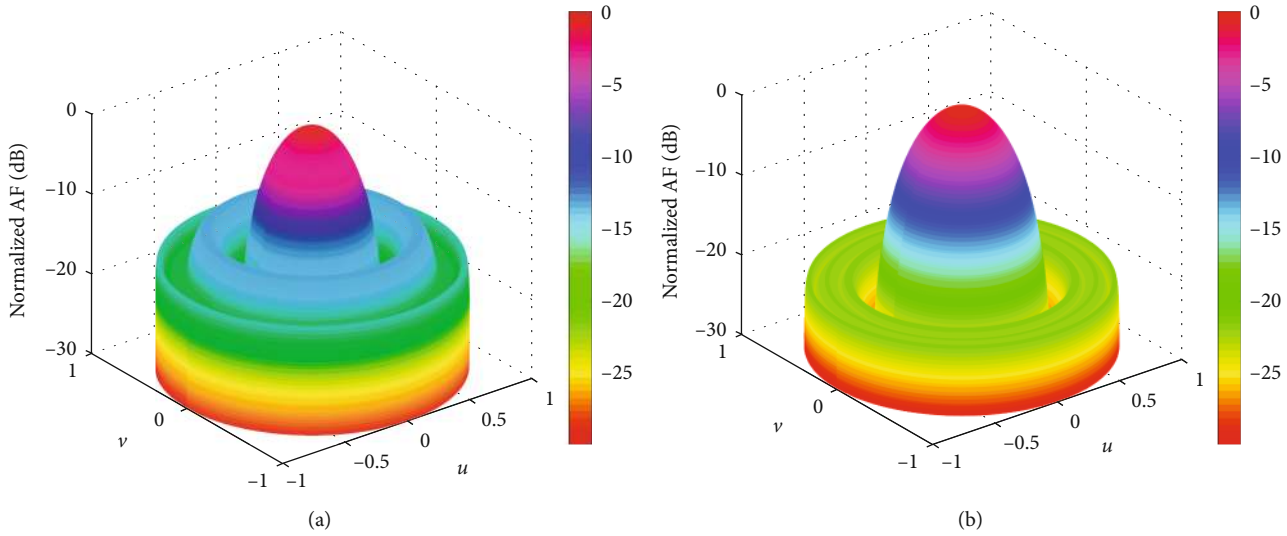

Figure 13: 3D radiation patterns of 8-element LAA before and after MSSA optimization: (a) before optimization; (b) after optimization.

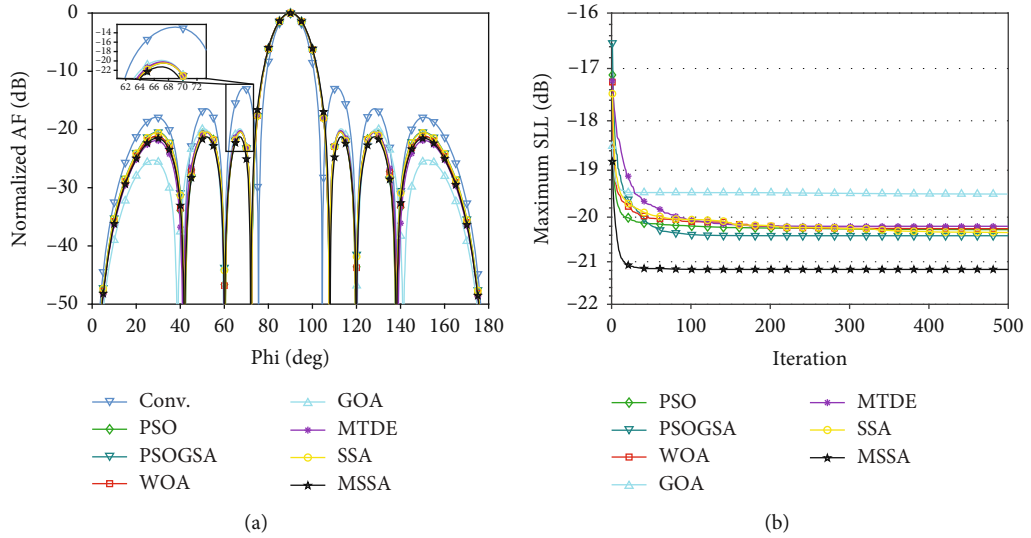

Figure 14: Beam patterns and convergence curves of 8-element LAA optimized by different algorithms: (a) beam patterns; (b) convergence curves.

Table 8: Optimized excitation amplitudes and maximum SLL of 8-element LAA by different algorithms.

Algorithm	Optimized excitation amplitudes (normalized)	Maximum SLL (dB)
Conv.	1.0000, 1.0000, 1.0000, 1.0000	-12.7972
PSO	1.0000, 0.8602, 0.6634, 0.5467	-20.2869
PSOGSA	1.0000, 0.8720, 0.6528, 0.5560	-20.4517
WOA	1.0000, 0.8618, 0.6618, 0.5462	-20.3507
GOA	1.0000, 0.8193, 0.7051, 0.4993	-19.8836
MTDE	1.0000, 0.8584, 0.6735, 0.5349	-20.1902
SSA	1.0000, 0.8702, 0.6544, 0.5542	-20.4375
MSSA	1.0000, 0.8636, 0.6424, 0.5128	-21.2569

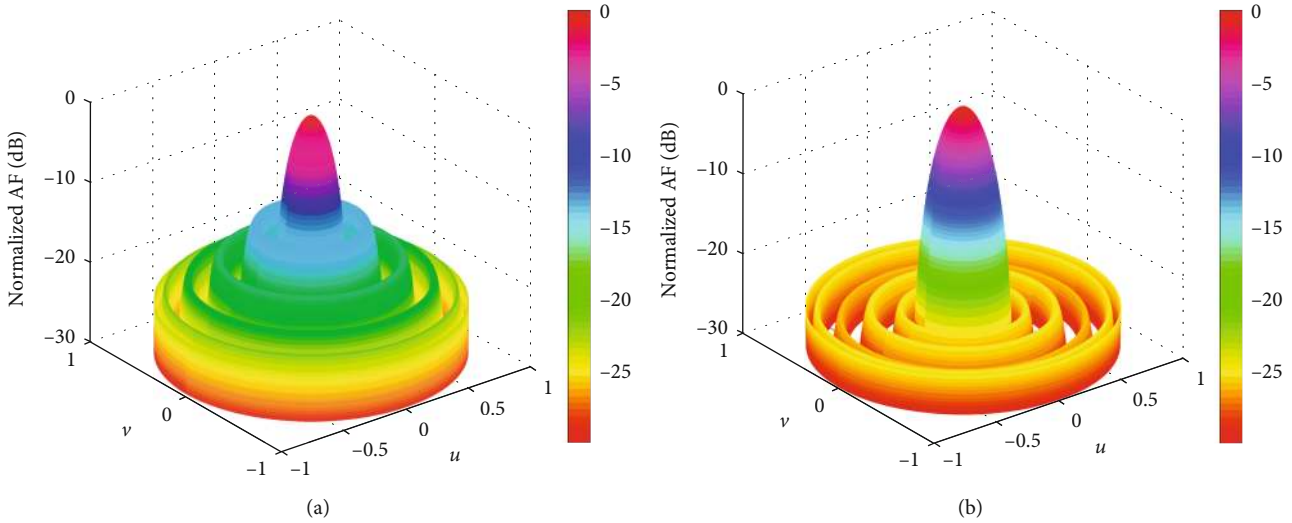

Figure 15: 3D radiation patterns of 16-element LAA before and after MSSA optimization: (a) before optimization; (b) after optimization.

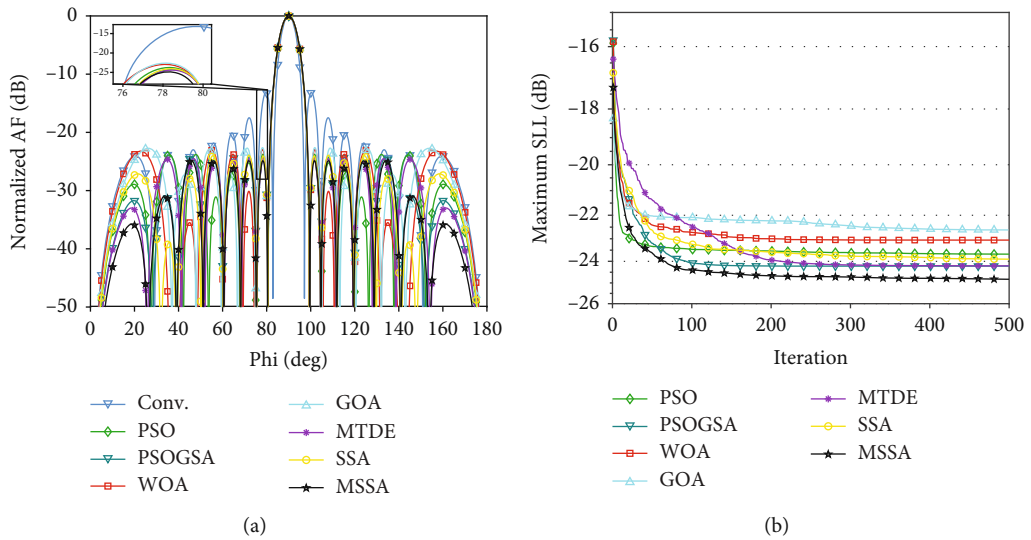

Figure 16: Beam patterns and convergence curves of 16-element LAA optimized by different algorithms: (a) beam patterns; (b) convergence curves.

Table 9: Optimized excitation amplitudes and maximum SLL of 16-element LAA by different algorithms.

Algorithm	Optimized excitation amplitudes (normalized)	Maximum SLL (dB)
Conv.	1.0000, 1.0000, 1.0000, 1.0000, 1.0000, 1.0000, 1.0000, 1.0000	-13.1476
PSO	1.0000, 1.0000, 0.9285, 0.7355, 0.7425, 0.5670, 0.4059, 0.4509	-23.7487
PSOGSA	1.0000, 0.9999, 0.8741, 0.8064, 0.6889, 0.4930, 0.5033, 0.4395	-24.2080
WOA	1.0000, 0.9809, 0.9023, 0.9761, 0.5847, 0.5656, 0.4604, 0.4002	-22.9487
GOA	1.0000, 0.8419, 0.8619, 0.7136, 0.7013, 0.4207, 0.5957, 0.2324	-22.6180
MTDE	1.0000, 0.9478, 0.9071, 0.7483, 0.7115, 0.4904, 0.4592, 0.4567	-24.4013
SSA	1.0000, 0.9652, 0.8346, 0.8395, 0.6237, 0.5275, 0.4877, 0.4115	-23.9233
MSSA	1.0000, 0.9711, 0.8581, 0.7839, 0.6875, 0.4687, 0.4784, 0.3895	-24.8687

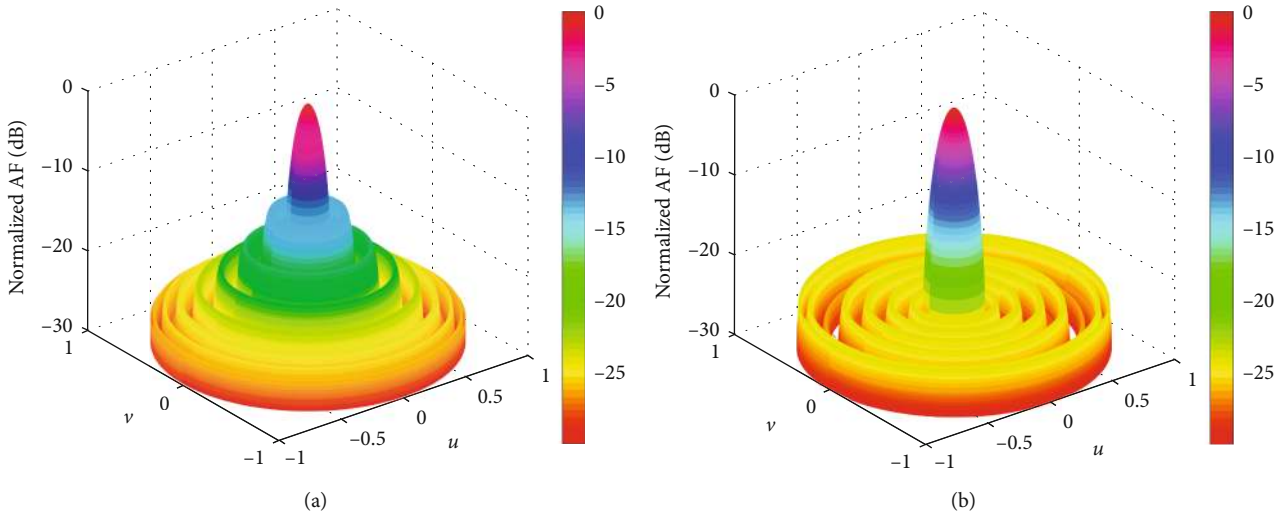

Figure 17: 3D radiation patterns of 24-element LAA before and after MSSA optimization: (a) before optimization; (b) after optimization.

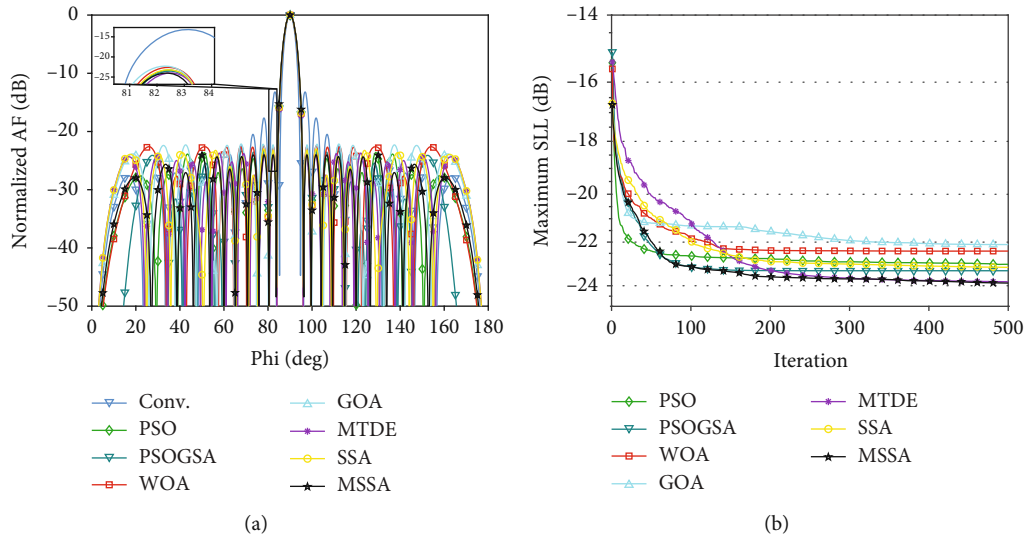

Figure 18: Beam patterns and convergence curves of 24-element LAA optimized by different algorithms: (a) beam patterns; (b) convergence curves.

Table 10: Optimized excitation amplitudes and maximum SLL of 24-element LAA by different algorithms.

Algorithm	Optimized excitation amplitudes (normalized)	Maximum SLL (dB)
Conv.	1.0000, 1.0000, 1.0000, 1.0000, 1.0000, 1.0000, 1.0000, 1.0000, 1.0000, 1.0000, 1.0000, 1.0000	-13.2091
PSO	1.0000, 1.0000, 1.0000, 0.8662, 0.8594, 0.7821, 0.6890, 0.5893, 0.6749, 0.3137, 0.6220, 0.4351	-23.1375
PSOGSA	1.0000, 0.9935, 0.9955, 0.7775, 0.9685, 0.7646, 0.7109, 0.5132, 0.5868, 0.4886, 0.5056, 0.4786	-23.3338
WOA	1.0000, 0.7820, 0.9905, 0.8429, 0.7500, 0.6529, 0.8972, 0.3259, 0.4892, 0.6179, 0.5064, 0.3145	-22.4755
GOA	1.0000, 1.0000, 0.9309, 0.7734, 0.7215, 0.9042, 0.7314, 0.4799, 0.6497, 0.3279, 0.6973, 0.2235	-22.1484
MTDE	1.0000, 0.8970, 0.8728, 0.8554, 0.7775, 0.7191, 0.7041, 0.6090, 0.4789, 0.4453, 0.3361, 0.6153	-23.7130
SSA	1.0000, 0.9598, 0.8152, 0.8919, 0.8345, 0.6096, 0.7762, 0.6822, 0.3127, 0.6130, 0.4044, 0.4461	-22.9933
MSSA	1.0000, 0.9979, 0.9066, 0.9165, 0.8683, 0.7488, 0.6761, 0.5852, 0.5815, 0.3026, 0.6685, 0.3467	-24.0121

Table 11: Statistical results of optimizing element position of 8-element LAA by different algorithms.

Maximum SLL (dB)	PSO	PSOGSA	WOA	GOA	MTDE	SSA	MSSA
Best	-19.7822	-19.5874	-19.6367	-19.8891	-19.8807	-19.8872	-20.2818
Worst	-18.1097	-16.6997	-16.4415	-15.4566	-17.2225	-18.1751	-18.4730
Mean	-19.0057	-19.4304	-18.6314	-18.4730	-19.6761	-19.5019	-20.0155
Std	0.3162	0.5932	0.8600	1.3805	0.5222	0.5069	0.4640

Table 12: Statistical results of optimizing element position of 16-element LAA by different algorithms.

Maximum SLL (dB)	PSO	PSOGSA	WOA	GOA	MTDE	SSA	MSSA
Best	-22.4235	-22.1479	-21.0826	-20.9566	-22.6257	-22.7315	-22.9611
Worst	-20.5435	-18.1108	-14.7938	-16.4117	-20.0713	-19.5287	-20.9210
Mean	-21.3471	-21.9683	-18.9752	-19.3923	-21.9622	-21.7445	-22.4318
Std	0.4310	0.7876	1.4892	1.5365	0.6582	0.8296	0.5563

Table 13: Statistical results of optimizing element position of 24-element LAA by different algorithms.

Maximum SLL (dB)	PSO	PSOGSA	WOA	GOA	MTDE	SSA	MSSA
Best	-22.0353	-22.9531	-19.8425	-22.9147	-24.1282	-24.1570	-24.2459
Worst	-19.6358	-20.4674	-15.9886	-16.2440	-21.3044	-21.1238	-22.1925
Mean	-20.9536	-22.4317	-17.7858	-19.4895	-23.1922	-22.8371	-23.7757
Std	0.5281	0.7872	1.0889	1.5849	0.8052	0.8865	0.6002

Table 14: Statistical results of optimizing excitation amplitude of 8-element LAA by different algorithms.

Maximum SLL (dB)	PSO	PSOGSA	WOA	GOA	MTDE	SSA	MSSA
Best	-20.4030	-20.4472	-20.4466	-20.4460	-20.4313	-20.4472	-21.2873
Worst	-19.5514	-19.5644	-19.6004	-17.5333	-19.9362	-19.6465	-20.5552
Mean	-20.2750	-20.4107	-20.2540	-19.5017	-20.2008	-20.3396	-21.1768
Std	0.1555	0.1729	0.2151	0.8734	0.0974	0.2032	0.1694

array and decreases successively to both sides. Such an amplitude distribution is feasible to the use of power dividers [14]. As can be observed in Table 8, the maximum SLL of conventional LAA is -12.7972 dB, and PSO, PSOGSA, WOA, GOA, MTDE, SSA, and MSSA are -20.2869 dB, -20.4517 dB, -20.3507 dB, -19.8836 dB, -20.1902 dB, -20.4375 dB, and -21.2569 dB, respectively. MSSA achieves the lowest SLL among these seven algorithms. The corresponding excitation amplitudes are also shown in Table 8.

4.3.2. 16-Element LAA. Figure 15 shows the 3D radiation patterns of 16-element LAA before and after MSSA

Table 15: Statistical results of optimizing excitation amplitude of 16-element LAA by different algorithms.

Maximum SLL (dB)	PSO	PSOGSA	WOA	GOA	MTDE	SSA	MSSA
Best	-24.0247	-24.5171	-23.8726	-24.3514	-24.4831	-24.4016	-25.4034
Worst	-23.2618	-23.8922	-21.9349	-21.0661	-23.9823	-22.8781	-24.1036
Mean	-23.6772	-24.2185	-23.0579	-22.6194	-24.2072	-23.9039	-24.8280
Std	0.2276	0.2007	0.5489	0.9146	0.1401	0.4476	0.3704

Table 16: Statistical results of optimizing excitation amplitude of 24-element LAA by different algorithms.

Maximum SLL (dB)	PSO	PSOGSA	WOA	GOA	MTDE	SSA	MSSA
Best	-23.3469	-23.8890	-23.4673	-23.7657	-24.0280	-23.9715	-24.5309
Worst	-22.3166	-21.8494	-20.8848	-20.2394	-23.4616	-22.0058	-22.8864
Mean	-22.9946	-23.2909	-22.3975	-22.1077	-23.8073	-23.1328	-23.8688
Std	0.2637	0.4853	0.6693	0.8942	0.1337	0.4787	0.4439

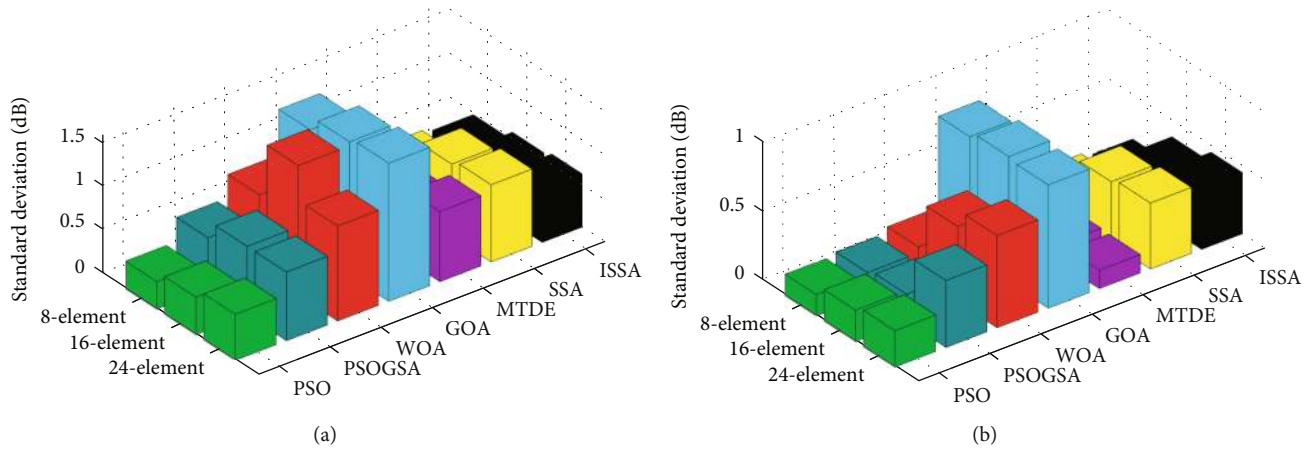

Figure 19: Standard deviation obtained by different algorithms: (a) element position optimization; (b) excitation amplitude optimization.

optimization. The beam patterns and convergence curves obtained by different algorithms are shown in Figure 16. It can be seen from Table 9 that the maximum SLL of PSO, PSOGSA, WOA, GOA, MTDE, SSA, and MSSA are reduced by 10.6011 dB, 11.0604 dB, 9.8011 dB, 9.4704 dB, 11.2537 dB, 10.7757 dB, and 11.7211 dB, respectively. Compared with conventional LAA, MSSA has the largest reduction. In addition, Table 9 also gives the optimized excitation amplitudes obtained by different algorithms.

4.3.3. 24-Element LAA. The 3D radiation patterns of 24-element LAA before and after MSSA optimization are depicted in Figure 17. Figure 18 is the beam patterns and convergence curves of 24-element LAA optimized by different algorithms. Table 10 shows the optimized element excitation amplitudes and maximum SLL. From the experimental results, the results of MSSA optimization are obviously better than those of the other six algorithms. This example further verifies the advantages of the modified algorithm in convergence speed as well as convergence accuracy.

4.4. Stability Test. Due to the randomness of the intelligent optimization algorithm, the results of each run are likely to be different, so it is necessary to discuss and analyze the stability of the algorithms. Similar to the performance analysis of the modified algorithm, Tables 11–16, respectively, give the best value, the worst value, the mean value, and the standard deviation of the maximum SLL obtained by different algorithms in optimizing the element position and excitation amplitude of the 8-element, 16-element, and 24-element LAA.

In order to visually display the fluctuation of data, the standard deviation diagrams of the element position and excitation amplitude optimized by different algorithms are drawn, as shown in Figure 19. According to the results of each run, the maximum SLL obtained by different algorithms are depicted in Figure 20. It is clear that, compared with the other six algorithms, the mean value of MSSA is the lowest, which indicates that the proposed algorithm has higher solution accuracy. The best value and the worst value are smaller than those of PSO, PSOGSA, WOA, GOA, MTDE, and SSA, which shows that the algorithm has strong optimization

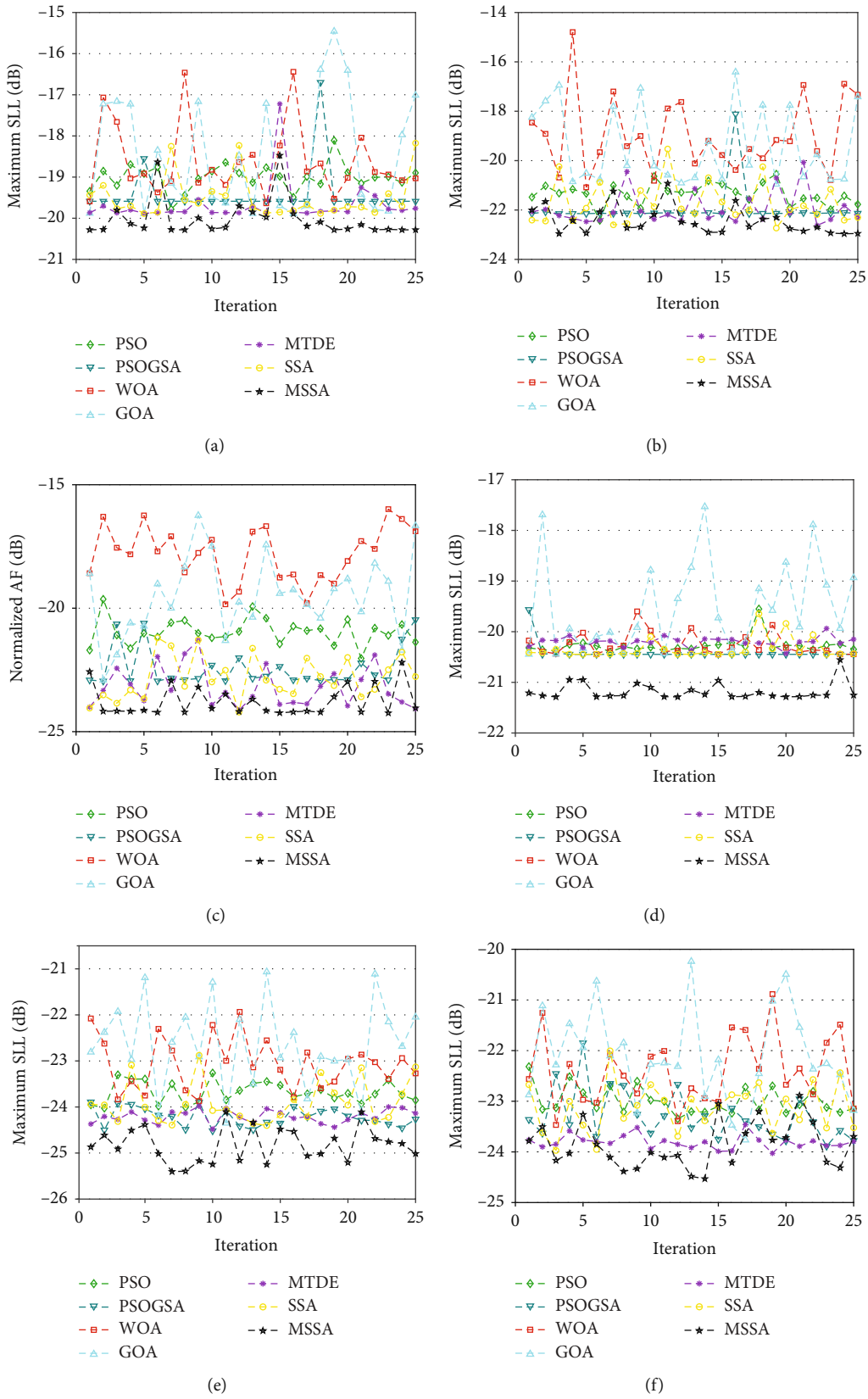

Figure 20: Result curves obtained by different algorithms: (a) 8-element position optimization; (b) 16-element position optimization; (c) 24-element position optimization; (d) 8-element excitation amplitude optimization; (e) 16-element excitation amplitude optimization; (f) 24-element excitation amplitude optimization.

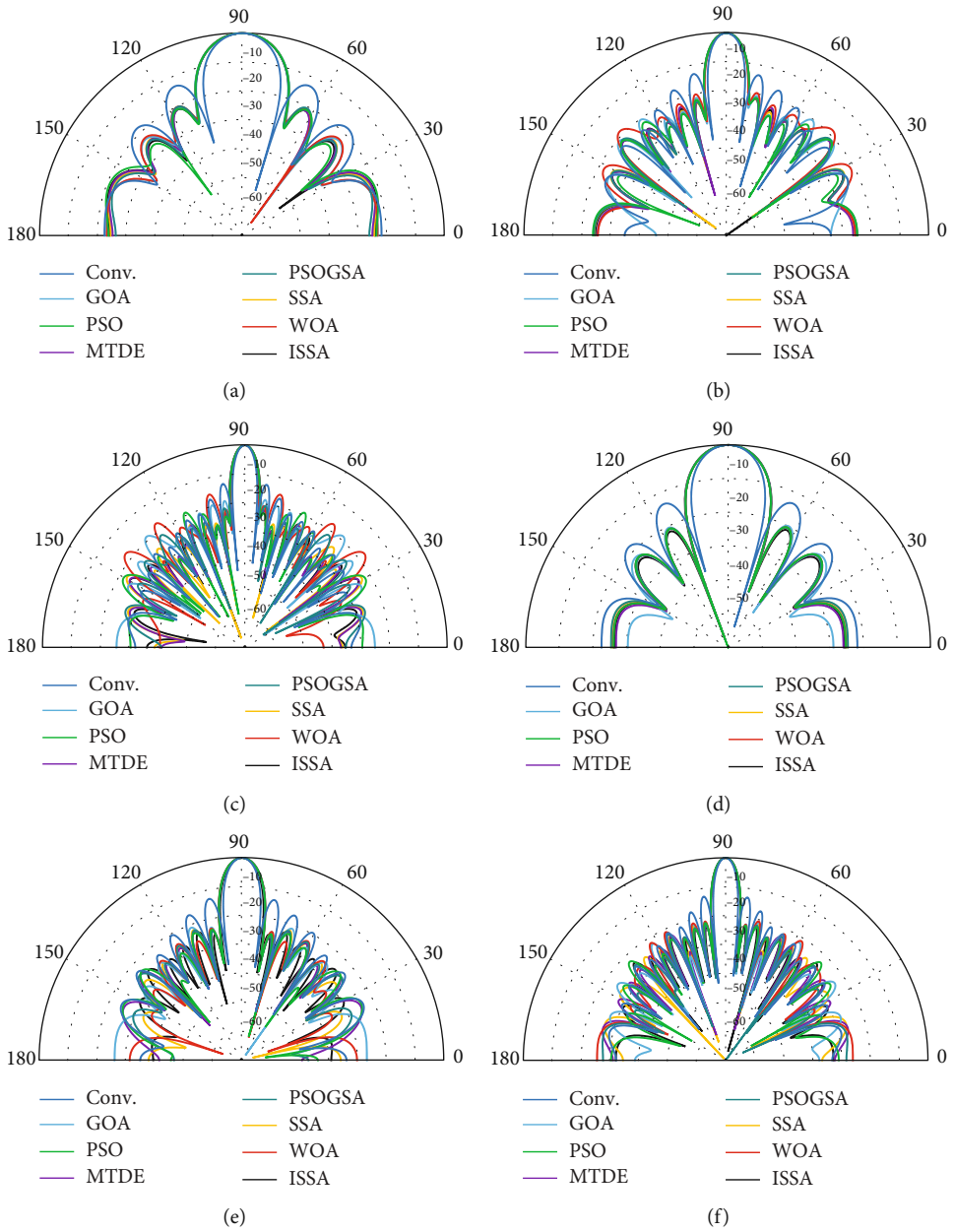

Figure 21: Polar coordinate patterns obtained by different algorithms: (a) 8-element position optimization; (b) 16-element position optimization; (c) 24-element position optimization; (d) 8-element excitation amplitude optimization; (e) 16-element excitation amplitude optimization; (f) 24-element excitation amplitude optimization.

Table 17: Maximum SLL of EM simulation in different scenarios.

	Conv.	PSO	PSOGSA	WOA	GOA	MTDE	SSA	MSSA
(a)	-13.2094	-20.8365	-20.2227	-20.1765	-20.3820	-20.9978	-20.9050	-21.0660
(b)	-13.0542	-21.2888	-21.0354	-18.2653	-20.2464	-21.4397	-21.3786	-21.6052
(c)	-12.9059	-18.9502	-20.4974	-15.6828	-18.4361	-22.0438	-21.6763	-22.1540
(d)	-13.2094	-20.3256	-20.4676	-20.3610	-19.8126	-20.1549	-20.4489	-21.1083
(e)	-13.0542	-23.0645	-22.2065	-22.9711	-20.9268	-22.5175	-21.9086	-23.2999
(f)	-12.9059	-21.9991	-22.1827	-20.6191	-21.1633	-22.6291	-21.6314	-22.8699

ability. Although MSSA stability is slightly inferior to that of the classical PSO algorithm and MTDE in excitation amplitude optimization, it performs better than the remaining algorithms.

4.5. EM Simulation. In practical applications, the induced current between elements will inevitably lead to mutual coupling. Conventional simulation, as a common processing mode in the most existing works on design of LAA for SLL reduction, usually assumes that array is in an ideal environment, and the effects of mutual coupling between the antenna elements are often ignored. EM simulation is an effective method to verify and evaluate the performance of different optimization algorithms in the actual environment [45]. With the help of EM simulation software Altair FEKO 2019, the actual LAA model is constructed firstly, and then, the 2D beam patterns of different antenna arrays in polar coordinates are obtained by simulation according to the above optimized element positions and excitation amplitudes. The beam patterns are shown in Figure 21. The numerical results of maximum SLL are listed in Table 17. It can be seen that the results of maximum SLL reduction are basically consistent with the above simulation results, which demonstrates that the algorithm is also effective for the practical conditions.

To sum up, based on the original algorithm, MSSA can give full play to the advantages of chaotic adaptive inertia weight and improved boundary constraint and enhance the global optimization ability. However, more work can be done to further enhance the stability and robustness of this algorithm. The numerical results of this paper indicate that the modified algorithm shows promise as an effective method in solving the global optimization problems.

5. Conclusions

In this paper, it is the first time that SSA and its modification have been introduced and utilized to the field of EM optimization according to the existing published literature and reports. For one thing, in order to improve the shortcomings of SSA, such as being easy to fall into local optimum and slow convergence speed, a novel modified SSA combining a homogeneous chaotic system, adaptive inertia weight, and improved boundary constraint is proposed. The computational results of three types of benchmark test functions verify the effectiveness of the modified algorithm. For the other thing, with the element positions and excitation amplitude as optimization variables and the maximum SLL reduction as optimization objective, a comparison with the classical PSO and PSOGSA, WOA, GOA, and MTDE through several scenarios is conducted. Simulation results show that MSSA achieved high performance in terms of maximum SLL reduction with a greater improvement in convergence accuracy, convergence speed, and stability. Therefore, SSA, as a new beam pattern optimization method for electromagnetic community and antenna design, has a large research space. In our future work, we will continue to study the algorithm and explore its real-world applications in the field of antenna array design, such as the multiobjective antenna array design problem aimed at minimizing at least two conflicting objectives at the same time, placing deep nulls of the beam pattern in desired directions to avoid the effect of jamming and interference, and other geometric configurations of the antenna array that work in different occasions.

Data Availability

The data used to support the findings of this study are included within the article.

Conflicts of Interest

The authors declare that there is no conflict of interest regarding the publication of this paper.

References

[1] H. Pradhan, B. B. Mangaraj, and S. K. Behera, "Antenna array optimization for smart antenna technology using whale optimization algorithm," in *2019 IEEE Indian Conference on Antennas and Propogation (InCAP)*, pp. 1–4, Ahmedabad, India, December 2019.

[2] J. Wang, Y. Nong, and Z. He, *Antenna Array Theory and Engineering Applications*, Publishing House of Electronics Industry, Beijing, 2015.

[3] G. Ram, D. Mandal, S. P. Ghoshal, and R. Kar, "Nature-inspired algorithm-based optimization for beamforming of linear antenna array system," in *Nature-Inspired Computing and Optimization*, pp. 185–215, Springer, 2017.

[4] B. Li, C. Liu, H. Wu, Y. Zhao, and Y. Dong, "Chaotic adaptive butterfly mating optimization and its applications in synthesis and structure optimization of antenna arrays," *International Journal of Antennas and Propagation*, vol. 2019, Article ID 1730868, 14 pages, 2019.

[5] M. A. Panduro, A. L. Mendez, R. Dominguez, and G. Romero, "Design of non-uniform circular antenna arrays for side lobe reduction using the method of genetic algorithms," *AEU-International Journal of Electronics and Communications*, vol. 60, no. 10, pp. 713–717, 2006.

[6] M. M. Khodier and C. G. Christodoulou, "Linear array geometry synthesis with minimum sidelobe level and null control using particle swarm optimization," *IEEE Transactions on Antennas & Propagation*, vol. 53, no. 8, pp. 2674–2679, 2005.

[7] K. Guney and M. Onay, "Bees algorithm for interference suppression of linear antenna arrays by controlling the phase-only and both the amplitude and phase," *Expert Systems with Applications*, vol. 37, no. 4, pp. 3129–3135, 2010.

[8] U. Singh, H. Kumar, and T. S. Kamal, "Linear array synthesis using biogeography based optimization," *Progress In Electromagnetics Research*, vol. 11, pp. 25–36, 2010.

[9] M. A. Zaman and M. Abdul Matin, "Nonuniformly spaced linear antenna array design using firefly algorithm," *International Journal of Microwave Science and Technology*, vol. 2012, Article ID 256759, 8 pages, 2012.

[10] L. Pappula and D. Ghosh, "Linear antenna array synthesis using cat swarm optimization," *AEU-International Journal of Electronics and Communications*, vol. 68, no. 6, pp. 540–549, 2014.

[11] U. Singh and M. Rattan, "Design of linear and circular antenna arrays using cuckoo optimization algorithm," *Progress in Electromagnetics Research*, vol. 46, pp. 1–11, 2014.

[12] K. Guney and A. Durmus, "Pattern nulling of linear antenna arrays using backtracking search optimization algorithm," *International Journal of Antennas and Propagation*, vol. 2015, Article ID 713080, 10 pages, 2015.

[13] N. I. Dib, "Design of linear antenna arrays with low side lobes level using symbiotic organisms search," *Progress In Electromagnetics Research*, vol. 68, pp. 55–71, 2016.

[14] P. Saxena and A. Kothari, "Optimal pattern synthesis of linear antenna array using grey wolf optimization algorithm," *International Journal of Antennas and Propagation*, vol. 2016, Article ID 1205970, 11 pages, 2016.

[15] R. Salgotra, U. Singh, and S. Sharma, "On the improvement in grey wolf optimization," *Neural Computing and Applications*, vol. 32, no. 8, pp. 3709–3748, 2020.

[16] H. Wu, Y. Yan, C. Liu, and J. Zhang, "Pattern synthesis of sparse linear arrays using spider monkey optimization," *IEICE Transactions on Communications*, vol. E100.B, no. 3, pp. 426–432, 2017.

[17] M. Hesari and A. Ebrahimzadeh, "Introducing deeper nulls and reduction of side-lobe level in linear and non-uniform planar antenna arrays using gravitational search algorithm," *Progress In Electromagnetics Research*, vol. 73, pp. 131–145, 2017.

[18] G. Sun, Y. Liu, H. Li, S. Liang, A. Wang, and B. Li, "An antenna array sidelobe level reduction approach through invasive weed optimization," *International Journal of Antennas and Propagation*, vol. 2018, Article ID 4867851, 16 pages, 2018.

[19] S. Mandal, "Linear antenna array pattern synthesis using elephant swarm water search algorithm," *International Journal of Information Engineering & Electronic Business*, vol. 11, no. 2, pp. 10–20, 2019.

[20] H. Wang, C. Liu, H. Wu, B. Li, and X. Xie, "Optimal pattern synthesis of linear array and broadband design of whip antenna using grasshopper optimization algorithm," *International Journal of Antennas and Propagation*, vol. 2020, Article ID 5904018, 14 pages, 2020.

[21] A. Durmus and R. Kurban, "Optimum design of linear and circular antenna arrays using equilibrium optimization algorithm," *International Journal of Microwave and Wireless Technologies*, pp. 1–12, 2021.

[22] D. H. Wolpert and W. G. Macready, "No free lunch theorems for optimization," *IEEE Transactions on Evolutionary Computation*, vol. 1, no. 1, pp. 67–82, 1997.

[23] J. Xue and B. Shen, "A novel swarm intelligence optimization approach: sparrow search algorithm," *Systems Science & Control Engineering*, vol. 8, no. 1, pp. 22–34, 2020.

[24] G. Liu, C. Shu, Z. Liang, B. Peng, and L. Cheng, "A modified sparrow search algorithm with application in 3d route planning for UAV," *Sensors*, vol. 21, no. 4, article 1224, 2021.

[25] H. Wang and J. Xianyu, "Optimal configuration of distributed generation based on sparrow search algorithm," *IOP Conference Series: Earth and Environmental Science*, vol. 647, no. 1, article 012053, 2021.

[26] Y. Wang and J. Tuo, "Blood glucose prediction based on empirical mode decomposition and SSA-KELM," in *2020 Chinese Automation Congress (CAC)*, pp. 4759–4763, Shanghai, China, November 2020.

[27] S. Kumaravel and V. Ponnusamy, "An efficient hybrid technique for power flow management in smart grid with renewable energy resources," *Energy Sources, Part A: Recovery, Utilization, and Environmental Effects*, pp. 1–21, 2020.

[28] J. Yuan, Z. Zhao, Y. Liu et al., "DMPPT control of photovoltaic microgrid based on improved sparrow search algorithm," *IEEE Access*, vol. 9, pp. 16623–16629, 2021.

[29] Y. Zhu and N. Yousefi, "Optimal parameter identification of PEMFC stacks using adaptive sparrow search algorithm," *International Journal of Hydrogen Energy*, vol. 46, no. 14, pp. 9541–9552, 2021.

[30] B. Liu and D. Rodriguez, "Renewable energy systems optimization by a new multi-objective optimization technique: a residential building," *Journal of Building Engineering*, vol. 35, article 102094, 2021.

[31] Y. Li, S. Wang, Q. Chen, and X. Wang, "Comparative study of several new swarm intelligence optimization algorithms," *Computer Engineering and Applications*, vol. 56, no. 22, pp. 1–12, 2020.

[32] C. Zhang and S. Ding, "A stochastic configuration network based on chaotic sparrow search algorithm," *Knowledge-Based Systems*, vol. 220, article 106924, 2021.

[33] S. Li and Y. Li, *Intelligent Optimization Algorithm Theory and Applications*, Publishing House of Harbin Institute of Technology, Harbin, 2012.

[34] A. Jovanović, L. Lazović, and V. Rubežić, "Adaptive array beamforming using a chaotic beamforming algorithm," *International Journal of Antennas and Propagation*, vol. 2016, Article ID 8354204, 8 pages, 2016.

[35] H. Zang, H. Huang, and H. Chai, "Homogenization method for the quadratic polynomial chaotic system," *Journal of Electronics & Information Technology*, vol. 41, no. 7, pp. 1618–1624, 2019.

[36] H. Yang, T. Chen, and N.-j. Huang, "An adaptive bird swarm algorithm with irregular random flight and its application," *Journal of Computational Science*, vol. 35, pp. 57–65, 2019.

[37] S. Cheng, Y. Shi, and Q. Qin, "Experimental study on boundary constraints handling in particle swarm optimization," *International Journal of Swarm Intelligence Research*, vol. 2, no. 3, pp. 43–69, 2011.

[38] J. Kennedy and R. Eberhart, "Particle swarm optimization," in *Proceedings of ICNN'95 - International Conference on Neural Networks*, pp. 1942–1948, Perth, WA, Australia, November-December 1995.

[39] Y. Shi and R. Eberhart, "A modified particle swarm optimizer," in *1998 IEEE International Conference on Evolutionary Computation Proceedings. IEEE World Congress on Computational Intelligence (Cat. No. 98TH8360)*, pp. 69–73, Anchorage, AK, USA, May 1998.

[40] S. Mirjalili and S. Z. M. Hashim, "A new hybrid PSOGSA algorithm for function optimization," in *2010 International Conference on Computer and Information Application*, pp. 374–377, Tianjin, China, December 2010.

[41] S. Mirjalili and A. Lewis, "The whale optimization algorithm," *Advances in Engineering Software*, vol. 95, pp. 51–67, 2016.

[42] S. Saremi, S. Mirjalili, and A. Lewis, "Grasshopper optimisation algorithm: theory and application," *Advances in Engineering Software*, vol. 105, pp. 30–47, 2017.

[43] M. H. Nadimi-Shahraki, S. Taghian, S. Mirjalili, and H. Faris, "MTDE: an effective multi-trial vector-based differential evolution algorithm and its applications for engineering design problems," *Applied Soft Computing*, vol. 97, article 106761, 2020.

[44] F. Gross, *Smart Antennas with MATLAB, Second Edition*, McGraw-Hill, 2015.

[45] G. Sun, Y. Liu, Z. Chen, S. Liang, A. Wang, and Y. Zhang, "Radiation beam pattern synthesis of concentric circular antenna arrays using hybrid approach based on cuckoo search," *IEEE Transactions on Antennas & Propagation*, vol. 66, no. 9, pp. 4563–4576, 2018.